Counteracting resistance to targeted therapy in melanoma by inhibiting discoidin domain receptors

Margaux Sala[1,2], Nathalie Allain[1,2], Elodie Henriet[1,2,#], Arnaud Uguen[1,3], Sylvaine Di-Tommaso[1,2,4], Anne-Aurélie Raymond[1,2,4], Jean-William Dupuy[5], Emilie Gerard[6], Nathalie Dugot-Senant[7], Benoit Rousseau[8], Jean-Phillipe Merlio[9,10], Anne Pham-Ledart[9,10], Béatrice Vergier[9,10], Violaine Moreau[1,2] and Frédéric Saltel[1,2,4]

[1]INSERM, UMR1053, BaRITOn, Bordeaux research in Translational Oncology, Team 1, 146 Rue Léo Saignat, Bordeaux, F-33076, France.
[2]Bordeaux University, 146 rue Léo Saignat, Bordeaux, F-33076, France.
[3]CHRU Brest, Department of Pathology, Brest, F-29200, France.
[4]Oncoprot, UMS 005, Bordeaux, F-33076, France.
[5]Univ.Bordeaux, Plateforme Protéome, Centre de Génomique Fonctionnelle, F-33000 Bordeaux, France
[6]CHU Bordeaux, Département de dermatologie, 1 avenue Jean Burguet, F-33000 Bordeaux, France.
[7]Plateforme d'histologie, UMS 005, Bordeaux, F-33076, France.
[8]Service commun des animaleries, Université de Bordeaux, F-33076.
[9] INSERM, UMR1053, BaRITOn, Bordeaux Research in Translational Oncology, Team 3, "Cutaneous Lymphoma Oncogenesis", 146 Rue Léo Saignat Bordeaux, F-33076, France.
[10] CHU Bordeaux, Tumor Bank and Tumor Biology Laboratory, Avenue de Magellan, Pessac, F-33604, France.

#present address: Ewald's lab-dpt of Cell biology, John Hopkins University school of Medicine, Baltimore
Keywords: melanoma, discoidin domain receptors, resistance, vemurafenib, dasatinib

Contact information:
Frédéric Saltel Ph.D.
INSERM, UMR1053, BaRITOn Bordeaux Research in Translational Oncology
146 rue Leo Saignat
33076 Bordeaux, France
E-mail: frederic.saltel@inserm.fr
Tel: +33 (0)5 57 57 17 07

Financial support:
This work is supported by Inca, SIRIC, Fondation de France, FRM.
Margaux Sala is supported by a PhD from the ministère supérieur de l'enseignement et de la recherche.

Abstract

Anti-BRAF plus an anti-MEK is currently used in first line for the management of patients presenting metastatic melanomas harboring the *BRAF V600E* mutation. However, the main issue during targeted therapy is the acquisition of cellular resistance in 80% of the patients, which is associated with an increased metastasis due to the hyperactivation of MAP kinase pathway. Previous reports have indicated that Discoidin Domain Receptors (DDRs) 1 and 2 can activate this pathway. To study the role of DDRs in melanoma cell resistance to targeted therapy, we first determined that DDRs are overexpressed in vemurafenib resistant cells compared to sensitive cells. We demonstrated that DDRs depletion or inactivation by DDRs inhibitors such as dasatinib or CR-13542 reduces tumor cell proliferation, due to a decrease of MAP kinase pathway activity in resistant cells. Finally, we confirmed these results *in vivo* in a xenograft mouse model and show that DDRs could be new therapeutic targets in resistant patients with metastatic melanoma. We propose that dasatinib could be a second-line treatment after the bi-therapy in resistant patients overexpressing DDRs.

Introduction

Melanoma, a malignant transformation of melanocytes, is the most aggressive form of skin cancer (Conde-Perez and Larue 2014). In 2018, it was predicted that there were 287 723 new melanoma cases were diagnosed worldwide and 60 712 deaths (Bray et al. 2018). Before 2011, the overall survival was six months; however, due to the development of combined targeted therapy and immunotherapy, it is now up to two years (Larkin et al. 2015; Long et al. 2015; Luke et al. 2017).

The most common type of cutaneous melanoma is Superficial Spreading Melanoma (SSM) which accounts for 70% of all melanomas (Elder et al. 2018). The *BRAF V600E* mutation is observed in almost 60% of SSM (Ascierto et al. 2012). The *BRAF* gene encodes a protein kinase involved in the MAP kinase pathway. Its mutation induces a constitutive activation of BRAF, leading to over-activation of the downstream signaling pathways, notably MEK and ERK. This in turn promotes anarchic cell proliferation and cell invasion in melanoma (Davies et al. 2002). During the past few years, therapies such as targeted bi-therapy or more recently immunotherapy have been developed. However, the response rate with immunotherapy is only 15% and a severe toxicity was observed in more than 25% of the patients (Luke et al. 2017). The combination of two treatments, an anti-BRAF plus an anti-MEK (vemurafenib and cobimetinib or dabrafenib and trametinib), is currently used as first line treatment in the management of patients with metastatic melanomas harboring the *BRAF V600E* somatic mutation (Larkin et al. 2015; Long et al. 2015). Vemurafenib and dabrafenib inhibit the activity of BRAF mutated protein whereas trametinib and cobimetinib inhibit MEK protein expression (Chapman et al. 2011; Flaherty et al. 2012; Hauschild et al. 2012). However, the main problem related to targeted therapy is the acquisition of cellular resistance in 80% of the patients, approximately two years after the treatment start (Sullivan and Flaherty 2013). This resistance is associated with an increased metastasis notably due to a hyperactivation of MAP kinase activity (Sullivan and Flaherty 2013). The hyperactivation of this signaling pathway could be due to genetic events including *NRAS* or *BRAF* mutations (Wagenaar et al. 2014), splice variation of *BRAF*, secondary mutation of *MEK*, overexpression of the oncoprotein BRAF or upregulation of tyrosine kinase receptors such as PDGFR, EGFR or FGFR (Basile et al. 2014; Du and Lovly 2018; Nazarian et al. 2010; Villanueva et al. 2010; Wagenaar et al. 2014).

Previous reports have indicated that Discoidin Domain Receptors (DDRs) 1 and 2 can also activate MAP kinase pathway (Chetoui et al. 2011; El Azreq et al. 2016; Ongusaha et al.

2003; Park et al. 2015; Ren et al. 2014; Valiathan et al. 2012a). DDRs belong to the tyrosine kinase receptor family and are composed of two members, DDR1 and DDR2 (Leitinger 2014). These transmembrane receptors are activated by collagens in their native triple helix form (Leitinger 2003; Shrivastava et al. 1997; Vogel et al. 1997) . DDR1 is activated for instance by type I and IV collagens whereas DDR2 preferentially binds type I, II and X collagens (Leitinger 2003; Leitinger and Kwan 2006; Shrivastava et al. 1997; Vogel et al. 1997). Moreover, DDRs are involved in several physiological functions and have been found overexpressed in a large number of cancer subtypes where they are associated with cell proliferation, invasion, migration and drug resistance (Badiola et al. 2011; Das et al. 2006a; Ezzoukhry et al. 2016; Juin et al. 2014; Malaguarnera et al. 2015; Nemoto et al. 1997; Payne and Huang 2014; Rudra-Ganguly et al. 2014; Xiao et al. 2015). DDR1 is involved in resistance to cancer therapy by activating Cox2 expression through NFκB pathways in breast cancer cells (Das et al. 2006b). DDR1 also promotes tumor cell resistance in lymphoma, ovarian cancer and glioblastoma cells (Ren et al. 2013, 2). Overexpression of DDR2 is associated with breast cancer recurrence through activation of the Erk/Snail 2 pathway (Ren et al. 2013, 2). In a recent study, binding of collagen 1A to integrins and DDR2 was shown to activate the Src-PI3K/Akt-NFκB signaling pathway, allowing the expression of apoptosis-inhibiting proteins (Rada et al. 2018). Thus, cisplatin-induced apoptosis was shown to be inhibited in ovarian cancer cells *in vitro* and *in vivo* (Rada et al. 2018).

The aim of this study is to fully determine whether DDRs could play a role in the resistance to combined therapy in melanoma. Moreover, we investigated if these receptors could be considered as new targets to counter this resistance process.

Here, we show overexpression of DDRs at protein levels in Vemurafenib resistant cell lines as compared to the sensitive ones. This overexpression is associated with an over activation of MAP kinase pathway. We report that depletion or inhibition of DDRs reduces tumor cell proliferation correlated with a decrease of MAP kinase pathway activity in resistant cells in 2D as well as in a 3D spheroid culture. We confirm these results *in vivo* in a xenograft mouse model and at clinical level in patient samples. Altogether, our data uncover an important role for DDRs in targeted therapy resistance in melanoma, and demonstrate that targeting those receptors could reduce tumor progression.

Results

DDRs are overexpressed in drug-resistant melanoma cells

To investigate whether DDR1 and DDR2 play a role in melanoma resistance, we determined their expression at mRNA and protein levels in melanoma resistant and sensitive cells. We used two pairs of melanoma cell lines: sensitive (229 S and 238 S) and resistant to vemurafenib (229 R and 238 R). The melanoma resistant cell lines derived from the sensitive *B-RAF* mutated cell lines by repeated vemurafenib treatment (Søndergaard et al. 2010). Resistance was maintained by adding vemurafenib to the culture medium at each passage. As mentioned in the introduction, resistance is associated to an hyperactivation of MAP kinase pathway activity. First, we confirmed that MAP kinase is overactivated in resistant cells compared to sensitive cells (**Figure 1A**). Second, there was an increase in DDR2 mRNA level in resistant cells compared to sensitive cells, whereas DDR1 mRNA level increased only in 238 R but not in 229 R cells (**Figure 1B**). In the study by *Nazarian et al*, DDR1 mRNA level did not increase in the 238 R and 229 R cells (Nazarian et al. 2010). However, at the protein level, we demonstrated that DDR1 and DDR2 are both overexpressed in resistant cells compared to sensitive ones (a 1.5-fold increase for DDR1 in both resistant cells lines whereas a 2-fold increase for DDR2 in 238R and a 6-fold increase in 229R) (**Figure 1C**). The overexpression in resistant cells was higher for DDR2 than for DDR1 compared to sensitive cells (**Figure 1C**).

Currently, melanoma patients are treated with the combination of a bi-therapy, hence, we measured DDRs expression in melanoma sensitive cells treated with vemurafenib, cobimetinib or both during two months. We demonstrated that sensitive cells treated 2 months with the bi-therapy exhibit a DDRs overexpression (**Figure 1D**) as shown for vemurafenib resistant cells. Most studies on the DDRs only focus on one of the two receptors; with these results, we demonstrated for the first time that melanoma resistant cells overexpressed both receptors. It is well characterized that DDRs are able to activate MAP kinase pathway (Valiathan et al. 2012b). As this signaling pathway is over-activated in patients with metastatic melanoma resistant to the currently used targeted therapy, we could hypothesize that resistant cell lines, despite the bi-therapy, are able to over-activate this pathway through DDRs overexpression and activation. To address this, we only focused on resistant cell lines in subsequent experiments.

DDRs are involved in MAP kinase pathway activation

In order to test the hypothesis that overactivation of MAP kinase pathway in resistant melanoma cells is due to DDRs overexpression, we analyzed the impact of DDRs depletion or DDRs kinase domain inactivation on this pathway. We quantified the effect of DDRs depletion by siRNA targeting DDR1, DDR2, or both, on MAP kinase pathway activity. We found that DDR1 and/or DDR2 silencing induced a decrease of PErk/Erk ratio in 238 R and 229 R cells (**Figure 2A, supplementary figure 1A**). Furthermore, we aimed to confirm this result by studying the impact of DDRs silencing on various MAP kinase targets at mRNA level such as PHLDA1 and ETV4. Indeed, DDR1 and/or DDR2 depletion induced a decrease of mRNA level of most of MAP kinase pathway targets (**Figure 2B, supplementary figure 1B**). To confirm these data and to bring this concept closer to a potential clinical use, we searched for FDA-approved drugs that inhibit kinase domains in both DDRs. We selected dasatinib, a multi-tyrosine kinase inhibitor which inhibits DDR1 and DDR2 kinase domains simultaneously at nanomolar range (Day et al. 2008). Moreover, dasatinib is currently employed in clinical practice for patients with chronic myeloid leukemia (Keating 2017). We observed that treating 238 R cells with 100 nM dasatinib for 2 hours inhibited, as expected, DDR1 and DDR2 auto-phosphorylation. In parallel, this treatment decreased the PErk/Erk ratio in vemurafenib-resistant melanoma cells (**Figure 2C, supplementary figure 1C**). This indicates that the kinase activity of DDRs is important for MAP kinase pathway activity in resistant cells. Altogether, these data demonstrate that DDRs are involved in MAP kinase pathway over-activation in resistant melanoma cell lines.

DDRs are involved in resistant tumor cell proliferation

As DDRs play a role in MAP kinase signaling pathway, we investigated the biological impact of DDRs inhibition on tumor cell proliferation. For this purpose, we analyzed the impact of DDRs silencing or kinase domain inhibition on cell proliferation, monitored in real time using IncuCyte® cell monitoring. First, we demonstrated that when DDR1, DDR2 or both are depleted using siRNA, there is a significant decrease of tumor cell proliferation in both resistant cell lines (**Figure 3A, supplementary figure 2A**). We also observed an inhibition of tumor cell proliferation when cells are treated with dasatinib at 100 nM (concentration where DDRs kinase activity is totally inactivated) compared to the control (**Figure 3B, supplementary figure 2B**). These results indicate that DDRs are required for cell proliferation in resistant melanoma cell lines. Overexpression of DDR2 is more pronounced than DDR1 in resistant cell lines compared to the sensitive cells (**Figure 1C**), hence, we decided to test the impact of DDR2 inhibition on cell proliferation. We transfected

melanoma resistant cells with wild-type DDR2 or DDR2 kinase-dead mutant (*K608E* mutation, named DDR2 KD). Transfecting cells with DDR2 KD mutant decreased cell proliferation as observed with dasatinib (**Figure 3C, supplementary figure 2C**). These results suggest that the effect observed with dasatinib is due to DDR2 inactivation. Recently, WRG28 was identified as a DDR2 allosteric and selective inhibitor (Grither and Longmore 2018). WRG28 acts via the extracellular domain of the receptor in an allosteric manner. It is highly selective and can dissociate preformed DDR2 collagen complex, disrupt receptor clustering in solution, inhibit kinase-independent receptor function. Based on this, and to confirm data obtained with the DDR2-KD mutant, we analyzed the impact of this DDR2 inhibitor on cell proliferation. Treatment of melanoma resistant cells with CR-13452, a WRG-28 analog, decreases DDR2 phosphorylation, ERK phosphorylation and consequently, inhibits cell proliferation, confirming the results previously obtained with dasatinib and kinase-dead experiments (**Figure 3D**). In this study, we used several ways to inhibit DDRs such as siRNA, dasatinib and a DDR2 inhibitor. To fully determine the role of DDRs in melanoma resistance to targeted therapy and the relevance of the dasatinib treatment in this context, it is important to investigate the effect of dasatinib in these melanoma resistant cells. Indeed, dasatinib is known to inhibit several targets such as Abl, DDR1, DDR2, Src. Of course, the Dasatinib impact depends on the concentration. We could observe a low and non-significant decrease of P Src expression in Dasatinib condition as compared to the control whereas there is a non-significant increase of P Src activity when treated with DDR2 inhibitor. We do not observe any difference on P Src expression between siControl and siDDR2 (**Supplementary Figure 2E).** We demonstrate that at this concentration, dasatinib blocks DDRs thereby decreasing cell proliferation in melanoma resistant cells. In addition to MAP kinase pathway, we analyzed by mass spectrometry the variations in protein expression following treatment of the 238R cells with dasatinib, DDR2 inhibitor or after transfection with siRNA targeting DDR2. By Gene set enrichment analysis (GSEA), we looked for the other commonly deregulated pathways under these 3 conditions showing that RhoA and EIF2 signaling are deregulated (**Supplementary figure 3**).

DDRs involvement in resistant tumor progression in 3D

To analyze DDRs role in physiological conditions, we tested the role of DDRs in cell proliferation using a 3D culture of spheroids. The resistant cells seeded in non-adherent conditions have the ability to form spheroids 72 h after seeding. To study the impact of dasatinib on spheroid maintenance, spheroids were treated with dasatinib at 100 nM, 72 h

after seeding. We observed a disruption of spheroids only in dasatinib condition (**Figure 4A, Supplementary figure 4A**). A quantification of the spheroid areas demonstrated that this area significantly decreased in the dasatinib condition (**Figure 4B, Supplementary figure 4B**). In order to verify whether the decrease in cell proliferation after dasatinib treatment is due to apoptosis, we monitored the Caspase 3/7 activity in 2D, on cells treated with dasatinib or not. We show that cells that have been treated with dasatinib are apoptotic, suggesting that dasatinib induces cell death in resistant melanoma cell lines (**Figure 4C, Supplementary figure 4C**). In order to validate these results on spheroid maintenance, we treated the spheroids 72 h after their formation with the DDR2 inhibitor CR-13452 (5 µM). Once again, we demonstrate that DDR2 inhibition led to an alteration of spheroid maintenance and to a decrease of its area (**Figure 4D&E**). We confirmed that cells that have been treated with DDR2 inhibitor are apoptotic in 2D, suggesting that DDR2 inhibitor induces cell death in resistant melanoma cell lines (**Figure 4F**).

Altogether, these data strongly suggest that DDRs are an important target in melanoma resistant cell proliferation and that they can be targeted by dasatinib or DDR2 inhibitor.

Role of DDRs in resistant tumor progression *in vivo*

An *in vivo* validation of the dasatinib effect is necessary to fully confirm its potential to target DDRs in melanoma cells resistant to vemurafenib. For that, we tested impact of dasatinib *in vivo*, in a xenograft mouse model of melanoma resistant cells. First, we subcutaneously implanted 229 R cells in NSG mice. When tumors reached 150 mm^3, animals were separated in two groups: one group treated with dasatinib and a control group still treated with vemurafenib by oral gavage (**Figure 5A**). When mice were treated with dasatinib, we observed a stabilization of tumor growth compared to the control group treated with vemurafenib, in which tumor growth dramatically increased (**Figure 5B & C**). A western blot analysis of mice tumors treated with dasatinib showed a decrease in DDR1 and DDR2 phosphorylation activity, as compared to a control mouse treated with vemurafenib (**Figure 5D**). These results indicate that dasatinib inhibited both DDR1 and 2 phosphorylation *in vivo*. Furthermore, we analyzed and compared tissue sections from mice tumor treated with dasatinib or vemurafenib. We observed necrotic areas in dasatinib treated mice compared to mice treated with vemurafenib (**Figure 5E**). We confirmed this result by Annexin V labeling, which is found in necrotic areas of dasatinib treated tumors (**Figure 5E**). This result is consistent with data obtained with spheroids (**Figure 4).** These results demonstrate that dasatinib has a pro-apoptotic activity in mice subcutaneously implanted with melanoma

vemurafenib resistant cells. In order to evaluate the clinical relevance of our results, we analyzed RNA sequencing database from 21 patients before and after treatment to dabrafenib which is an anti-BRAF. The data are provided from Gene Expression Omnibus (accession number: GSE50509). We studied abundance of DDR1, DDR2 or both, before and after treatment with dabrafenib. Following dabrafenib treatment, DDR1 is overexpressed in 38% of the cases, while DDR2 is overexpressed in 24% of the cases. Moreover, very importantly, we observed an overexpression of DDR1, DDR2, or both in 80% of the cases (**Figure 5F)**. All these findings correlate with our *in vitro* data and highlight that DDR1 and DDR2 could be new therapeutic targets in patients with metastatic melanoma resistant to anti-BRAF therapies. Dasatinib could then be clinically used in resistant patients following targeted dual therapy and who are not included in an immunotherapy protocol.

Discussion

When patients develop metastatic melanoma harboring the *BRAF V600E* mutation, the first line of treatment corresponds to a targeted bi-therapy with anti-BRAF and anti-MEK. However, 80% of the cases become resistant to this treatment, approximatively after 2 years(Larkin et al. 2015; Long et al. 2015). Resistance to BRAF in melanoma leads to an over-activation of MAP kinase pathway which could be due to different alterations, either genetic or epigenetic, including overexpression of tyrosine kinase receptors such as PDGFRβ or EGFR (Nazarian et al. 2010; Sullivan and Flaherty 2013). Over the past few years, it has been established that DDRs, including DDR1 and DDR2, activate MAP kinase pathway (Chetoui et al. 2011; Conde-Perez and Larue 2014; El Azreq et al. 2016; Ongusaha et al. 2003; Park et al. 2015; Ren et al. 2014; Valiathan et al. 2012a). Herein, we demonstrated that DDR2 is overexpressed at mRNA and protein levels in two vemurafenib-resistant melanoma cell lines compared to sensitive ones, while DDR1 increased only in 238 R cells at the protein level. The difference between DDR1 protein and mRNA levels in 229 R cells could be explained by the fact that DDR1 expression can be post transcriptionally regulated by microRNA, for instance (Deng et al. 2017a). It could be then interesting to study if there is any DDR1 regulation by microRNA in melanoma resistant cells. However, DDR2 seems to be more overexpressed than DDR1 in melanoma resistant cells compared to the sensitive cells. It could maybe due to the fact that melanoma resistant cells secreted their own matrix. Indeed, we demonstrated in our lab, that DDR1 expression is reduced when the cells are seeded on collagen I, whereas *Sekiya et al* showed that, in stellar hepatic cells, DDR2 mRNA can be decreased by microRNA-29b, which targets collagen I, suggesting a relationship between collagen I expression and DDR2 (Sekiya et al. 2011). Furthermore, as the microenvironment plays a critical role in melanoma resistance to vemurafenib, it would be then interesting to study DDRs expression in stromal cells(Chetoui et al. 2011; El Azreq et al. 2016; Ongusaha et al. 2003; Park et al. 2015; Ren et al. 2014; Valiathan et al. 2012a); DDR1 and DDR2 expression was observed in stromal cells in other cancers promoting cell invasion and metastasis formation (Corsa et al. 2016; Gonzalez et al. 2017; Jin et al. 2018). At the clinical level, we found that abundance of DDR1, DDR2 or both increases after treatment to an anti-BRAF, confirming the results obtained *in vitro*.

DDRs are major players in cancer progression and are associated with a bad prognosis when overexpressed (Henriet et al. 2018; Valiathan et al. 2012a). It was demonstrated that

DDR1 expression in melanoma lesions correlates with poor prognosis (Reger de Moura et al. 2019). Furthermore, different studies demonstrated a role of DDR1 in resistance in breast cancer, ovarian cancer and glioblastoma cells (Aljohani et al. 2015; Das et al. 2006a; Deng et al. 2017b). In breast cancer, DDR1 was shown to be one of the tyrosine kinase receptors involved in resistance to MEK inhibition. Thus, DDR1 depletion restores MEK inhibitor sensitivity in breast cancer cells (Duncan et al. 2012). Contrary to DDR1, little is known about the role of DDR2 in the acquisition of tumor cell resistance to chemotherapy. For the first time, we highlight an important role of DDR2 in resistance to vemurafenib demonstrating that in resistant melanoma cells, DDRs induce an overactivation of MAP kinase pathway, promoting proliferation.

We demonstrated that DDRs depletion reduced tumoral cell proliferation by reducing MAP kinase pathway activity. To test its clinical relevance, we selected dasatinib, an FDA-approved kinase domain inhibitor in chronic myeloid leukemia (Keating 2017). Dasatinib is also known as an inhibitor of SRC, which is engaged in a regulatory loop with DDRs (Day et al. 2008). We demonstrated that DDRs inactivation by dasatinib inhibits melanoma cell proliferation *in vitro*. As DDR2 is five-times more overexpressed than DDR1 in resistant cells compared to sensitives cells, we focused on this receptor first. DDR2 acts as a major player of tumor progression, migration and proliferation in melanoma (Badiola et al. 2011; Poudel, Lee, and Kim 2015). We confirmed results obtained with dasatinib, by using a DDR2 kinase-dead mutant and a selective DDR2 inhibitor. All promoted a decrease of tumoral cell proliferation suggesting that effect observed with dasatinib is mainly due to DDR2. Furthermore, by proteomic analysis, we demonstrated that DDR2 depletion with siRNA, DDR2 selective inhibition or Dasatinib treatment induce a decrease of RhoA signaling. Thoese results confirmed the recent study of *Misek et al*, which showed that in resistant cells there is an accumulation of actin stress fiber due to RhoA activation (Misek et al. 2019).

We demonstrated that inactivation of DDRs, or specifically DDR2 inhibition, promotes alteration of the spheroid maintenance by disruption of the cells (in 3D) and inducing cell apoptosis (in 2D). It could be relevant to study DDRs localization in these conditions as DDR1 is known to play a role in cell-cell junctions whereas there has been no reports on this role for DDR2 (Hidalgo-Carcedo et al. 2011). Indeed, DDRs can be present in various subcellular compartments associated with several cellular processes involved in cancer progression (Henriet et al. 2018). For example, DDR1 and DDR2 co-localize along the same fiber of collagen I (Henriet et al. 2018).

To confirm our result *in vivo*, we validated dasatinib effect in a xenograft mouse model and observed that dasatinib blocks tumor proliferation of vemurafenib-resistant melanoma cells. Sequential treatment is a crucial question in clinic to abrogate the toxicity due to therapy combination or to alternate treatments (Wang et al. 2018). Currently, a study demonstrated that switching from MAPK inhibitor therapy to vorinostat, is more effective in eradicating drug-resistant cells than a drug holiday (Wang et al. 2018). In this respect, we could study the effect of sequential treatment, in long term, in order to delay the apparition of resistance to vemurafenib or dasatinib (Wang et al. 2018).

We demonstrated that DDRs could be a good target in melanoma resistance to targeted therapy. DDRs may be targeted using FDA-approved tyrosine kinase receptor inhibitors such as dasatinib, imatinib, nilotinib with an IC50 in the low nanomolar range (Day et al. 2008). Nilotinib and dasatinib are more potent than imatinib toward DDR1 and DDR2 (Day et al. 2008). The IC50 for dasatinib is 0.5 nM for DDR1 and 1.4 nM for DDR2 whereas the IC50 for nilotinib is 43 nM for DDR1 and 55 nM for DDR2 (Rammal et al. 2016). In clinic, it will be more relevant to use dasatinib compared to nilotinib, due to its high affinity for DDRs and lower concentration could reduce treatment toxicity. Furthermore, dasatinib efficiency has been proven in different cancer types such as lung, gastric, head and neck and lung adenocarcinoma (Ambrogio et al. 2016; Hammerman et al. 2011; Hedberg et al. 2016; Kurashige et al. 2016; Pitini et al. 2013). However, these tyrosine kinase inhibitors are not DDRs-specific or not specific at all. In recent years, selective DDR inhibitors emerged. For instance, DDR1 could be targeted specifically by a pyrazolopyramidine alkyne derivative (7rh and 7rj), by DDR1-IN-1 or DDR1-IN-2 (Gao et al. 2013; Kim et al. 2013). The efficiency of 7rh has been proven by the tumor regression in xenograft mouse model of pancreatic ductal carcinoma lung adenocarcinoma, nasopharyngeal carcinoma and gastric cancer (Aguilera et al. 2017; Ambrogio et al. 2016; Lu et al. 2016). Regarding DDR2, Pr Longmore's team developed WRG28 (and an analog CR-13452), a selective DDR2 inhibitors used in our which acts via the extracellular domain of the receptor in an allosteric manner (Grither and Longmore 2018). However, the emergence in recent years of small molecules or inhibitors that specifically target DDRs could potentially help developing drugs to treat cancers.

We were able to demonstrate that DDRs are good targets in melanoma cells, which have secondary resistance against vemurafenib. In order to establish a correlation between DDRs overexpression and the three types of resistance that exist, good responders (10%), primary resistance (10%) and secondary resistance (80%) a perspective should be to measure

DDRs expression in those conditions. Finally, analysis of patient biopsies - in all three categories of responders - for DDRs expression could be informative. This strategy could determine DDRs as biomarkers of primary and/or secondary resistance in melanoma. However, due to the difficulty to obtain reproducible data for DDRs on IHC, this approach would be complex.

To summarize, in this study, we uncovered an important role for DDRs in tumoral proliferation for resistant patients with metastatic melanoma. Moreover, we propose dasatinib as a second line treatment after the targeted bi-therapy in resistant patients overexpressing DDRs.

Material and methods

Cell culture

Human melanoma cell lines 229 or 238 with *BRAF V600E* mutation were used from *Nazarian et al. 2010* (Nazarian et al. 2010). These cell lines were a generous gift from Dr Sophie Tartare-Deckert (U1065, Nice). The resistant cells (named 229 R and 238 R) derived from the sensitive ones (named 229 S and 238 S) by Vemurafenib treatment (Søndergaard et al. 2010). Both sensitive and resistant cell lines, 229S/R and 238S/R, were cultured in Dulbecco's modified Eagle's medium with 4.5 g/l glucose Glutamax-I (Invitrogen) supplemented with 10% fetal calf serum (Sigma-Aldrich). The resistance was maintained by addition of 1 µM of vemurafenib *(LC Laboratories*) to the medium. In each experiment with resistant cells, vemurafenib is added every day.

Reagents and drugs

Collagen polymerization was carried out as described previously (*Juin et al., 2012*). In brief, collagen was diluted at 0.5 mg/ml in DPBS 1X, then polymerized for 4 h at 37 °C before cell seeding. Cells were seeded for 4 h on collagen before fixation.

Vemurafenib and dasatinib were purchased from LC laboratories. DDR2 inhibitor (CR-13452) was a generous gift from Pr. Gregory Longmore Lab.

Western Blot

Protein cell lysates were obtained in radio-immunoprecipitation assay buffer (25 mM Tris HCl, pH 7.5, 150 mM NaCl, 1% IGEPAL, 1% sodium deoxycholate, and 0.1% SDS) completed with protease and phosphatase inhibitors. Proteins were blotted on a nitrocellulose membrane (Transblot® TurboTM midi-size, Bio-Rad), blocked with the Odyssey blocking buffer (LI-COR Company), and probed with primary antibodies overnight at 4°C. The following antibodies were used: rabbit monoclonal anti-DDR1 (5583S, cell signaling); rabbit monoclonal anti-DDR2 (12133S, Cell signaling); rabbit monoclonal anti-P-DDR1 (14531, cell signaling), rabbit monoclonal anti-P-DDR2 (MAB25382, R&D Systems), mouse monoclonal anti-P-Erk (9106S, Cell signaling); rabbit monoclonal anti-Erk (9102S, Cell signaling); rabbit monoclonal anti-P-Akt (2965S, Cell signaling), rabbit monoclonal anti-Akt (9272S, cell signaling), mouse monoclonal anti-P-Src (Milipore, 5677), rabbit monoclonal anti-Src (Milipore 4772), mouse monoclonal anti-Myc (Santa Cruz, sc-40) and mouse monoclonal anti-GAPDH (sc-166545, Santa Cruz Biotechnology) diluted in Tris buffered

saline (TBS) 5% bovine serum albumin (BSA). After washing with TBS 0.1% Tween (twice for 10 minutes), the membrane was incubated for 1 h with the fluorescent far-red coupled secondary antibody, in accordance with the primary antibody: IRDye 680RD goat (polyclonal) anti-rabbit IgG (H+L), (LI-COR) or IRDye 800RD goat (polyclonal) anti-mouse IgG (H+L), (LI-COR), diluted 1:5000 in TBS 5% BSA. After washing twice for 10 minutes with TBS 0.1% Tween and with 1x TBS, membranes were revealed with the BioRad imager with the Image studio software as recommended by the manufacturer. Quantification of the correct size band for each antibody was performed with the ImageLab software.

Transfections

Small interfering RNAs (siRNA) (20 nM) were transfected using Lipofectamine RNAiMax (Invitrogen) according to the manufacturer's instructions. The siRNA sequences targeting human DDR1 and DDR2 were as follows: siDDR1 5′-GAAUGUCGCUUCCGGCGUGUU-3', siDDR2 5'-GAAACUGUUUAGUGGGUAA-3'. A control siRNA targeting luciferase (CT) 5′-CGTACGCGGAATACTTCGA-3′ was purchased from Eurofins MWG Operon, Inc. The efficiency of the silencing was determined using western blotting and reverse transcription-quantitative polymerase chain reaction (RT-qPCR). For DNA transfection, $2*10^5$ cells were seeded on 6 well cultured plates and transfection with DDR2-KD (generously given by Dr Jin Su.) the following day with 1 µg using Jetprime (Polyplus transfection) following the manufacturer's instructions. Experiments were performed 72 hours after transfection.

RT-qPCR

mRNAs were extracted from culture cells using the kit Nucleospin RNA® from Macherey Nagel according to the manufacturer's instructions. cDNA was synthetized from 1 µg of total RNA with maxima reverse transcriptase (Fermentas). Around 30 ng of cDNA were then subjected to PCR amplification on quantitative Real-Time PCR system using the CFX96 Real Time PCR detection system (Biorad). The SYBR® Green SuperMix for iQTM (Quanta Biosciences, Inc.) was used with the following PCR amplification cycles: initial denaturation, 95 °C for 10 min, followed by 40 cycles with denaturation, 95 °C for 15 s and annealing extension, 60 °C for 1 min. Gene expression results were first normalized to internal control with RNA ribosomal 18S. Relative levels of expression were calculated using the comparative (2-ΔΔCT) method. All primers used for qRT-PCR experiments are listed in supplementary Table 1.

IncuCyte® assays

Proliferation assays: Cells were seeded in a 96-well plate (at 5 000 cells per well) and then monitored by the videomicroscope IncuCyte® (Essen Bioscience). Cell confluence and quantification was done using IncuCyte® imaging system. For dasatinib experiments, the dasatinib was added at 100 nM. **Apoptotic assays:** 229 R and 238 R cells were seeded at a density of 5 000 cells per well and allowed to grow overnight. The next day, dasatinib (100 nM) was prepared and added, directly followed by the caspase 3/7 reagent in final dilution of 1/1000. Cells were then incubated in IncuCyte® Zoom live cell imaging. The IncuCyte® Caspase-3/7 apoptosis assay green reagent couples the activated caspase-3/7 recognition motif (DEVD) to NucView™ 488, a DNA intercalating dye to enable quantification of apoptosis over time. **Spheroid assays**: Cells were seeded into a 96-well ultra-low attachment plate. Then, we monitored spheroid formation using IncuCyte® videomicroscopy for 72 h. After spheroid formation, the treatment (dasatinib or CR-13452) was added. The quantifications of spheroid area and perimeter were performed using Image J.

Proteomic analysis

Cell lysis was performed in RIPA Buffer. The steps of sample preparation and protein digestion were performed as previously described (Henriet et al. 2017). NanoLC-MS/MS analysis were performed using an Ultimate 3000 RSLC Nano-UPHLC system (Thermo Scientific, USA) coupled to a nanospray Orbitrap Fusion™ Lumos™ Tribrid™ Mass Spectrometer (Thermo Fisher Scientific, California, USA). Mascot 2.5 software was used for protein identification in batch mode by searching against the UniProt Homo sapiens database (74 489 entries, Reference Proteome Set, release date: May 16, 2019) from http://www.uniprot.org/ website. Raw LC-MS/MS data were imported in Proline Studio (http://proline.profiproteomics.fr/) for feature detection, alignment, and quantification. Proteins identification was accepted only with at least 2 specific peptides with a pretty rank=1 and with a protein FDR value less than 1.0% calculated using the “decoy” option in Mascot. Label-free quantification of MS1 level by extracted ion chromatograms (XIC) was carried out with parameters indicated previously (Henriet et al. 2017). Protein ratios were median normalized.

Gene Set Enrichment Analysis was performed against the Ingenuity Pathways Database (Canonical Pathways). Only commonly and significantly deregulated pathways were considered.

Xenograft mouse model

The institutional animal ethics committee of Bordeaux University approved all animal use procedures and all efforts were made to minimize animal suffering. Five million 229 R cells were resuspended in a mixed 1:1 with DMEM 4.5 g/l glucose Glutamax-I medium and matrigel. The mixture was then injected subcutaneously into the right flank of anesthetized 8 weeks-old NOD/LtSz-*scid* IL2Rγ*null* (NSG) mouse. Tumor formation and tumor volume, based on caliper measurements, were monitored twice a week. The mice were treated with vemurafenib. until the tumors reached approximately 150 mm^3 in volume. Subsequently, the mice were randomly assigned in 2 groups: one control group where mice were treated with vemurafenib (40 mg/kg) by oral gavage, and one group where mice were treated with dasatinib (20 mg/kg) by oral gavage (n=5 in each condition).

Immunohistochemistry

Primary tumors were fixed in 10% buffered formaldehyde. Selected representative slides including treated tumors with dasatinib or not treated tumors were processed for Annexin V immunohistochemistry (IHC). The 2.5 µm thick sections were dewaxed and rehydrated and antigen was retrieved in a sodium citrate buffer (pH6 solution for 20 mins). All staining procedures were performed in an automated autostainer (Dako-Agilent Clara, United States) using standard reagents provided by the manufacturer. The sections were incubated with an anti-Annexin V (Abcam, ab14196) rabbit polyclonal antibody (16210-1-AP; ProteinTech) at a 1µg/ml dilution for 45 min at room temperature. EnVision Flex/HRP (Horseradish peroxidase) (Dako-Agilent, 20 minutes) was used for signal amplification. 3,3'-Diamino-benzidine (DAB, Dako) development was used for detecting primary antibodies. The slides were counterstained with hematoxylin, dehydrated and mounted. Each immunohistochemical run contained a negative control (buffer, no primary antibody). Sections were visualized with a Nikon-Eclipse501 microscope, and images were acquired using NIS-Elements F.

Statistical Analysis

Data were reported as the mean ± SEM of at least three experiments. Statistical analyses were performed using GraphPad Prism 5.0. The differential protein expression between the cell lines was validated by a t test * $p<0.05$. One-way ANOVA analysis of variance followed by

Bonferroni post-test was used for the comparison of means in experiments containing three groups or more * P0.05, ** P≤0.01, *** P≤0.001.

Data availability section

RNA seq data: gene expression
Omnibus GSE50509 (https://www.ncbi.nlm.nih.gov/geo/query/acc.cgi?acc=GSE50509)

Acknowledgements

We are grateful to Pr Longmore who provided DDR2 inhibitor. Many thanks to Dr David Santamaria who gave advices on this project and provided list of MAP kinase target and their associated primers. We are grateful to Dr Sopie Tartare-Deckert who provided melanoma cells.

Authors contribution

Study concept and design, analysis and interpretation of data, writing the paper: Margaux Sala and Frédéric Saltel. Acquisition of data: Margaux Sala (*in vitro* experiments), Nathalie Allain (mouse model), Arnaud Uguen (immunohistochemistry analysis), Nathalie Dugot-Senant (immuhistochemistry technical support). Sylvaine Di-Tommaso, Jean-William Dupuy, Anne-Aurélie Raymond mass spectrometry-based proteomic analysis.

Conflicts of interest

The authors declare that they have no conflict of interest.

The paper explained

Problem

Melanoma is an aggressive form of skin cancer with a poor prognosis when treated late. Despite the recent progress of patient management presenting metastatic melanomas, the main issue is the acquisition of cellular resistance in 80% of the patients. Indeed, there is an urgency to identify novel targets and new therapeutic strategies in melanoma resistance.

Results

We demonstrated that DDRs depletion or inactivation by DDRs inhibitors such as dasatinib or CR-13542 reduces tumor cell proliferation, due to a decrease of MAP kinase pathway activity in resistant cells *in vivo* and *in vitro*. We showed that DDRs could be new therapeutic targets in resistant patients with metastatic melanoma.

Impact

Our results may show that DDRs are crucial targets in melanoma resistance. We propose Dasatinib as a second-line treatment after targeted dual therapy in resistant patients overexpressing DDRs.

For more information

RNA seq data: gene expression
Omnibus GSE50509 (https://www.ncbi.nlm.nih.gov/geo/query/acc.cgi?acc=GSE50509)

References

Aguilera, Kristina Y., Huocong Huang, Wenting Du, Moriah M. Hagopian, Zhen Wang, Stefan Hinz, Tae Hyun Hwang, et al. 2017. 'Inhibition of Discoidin Domain Receptor 1 Reduces Collagen-Mediated Tumorigenicity in Pancreatic Ductal Adenocarcinoma'. *Molecular Cancer Therapeutics* 16 (11): 2473–85. https://doi.org/10.1158/1535-7163.MCT-16-0834.

Aljohani, Hashim, Robert F. Koncar, Ahmad Zarzour, Byung Sun Park, So Ha Lee, and El Mustapha Bahassi. 2015. 'ROS1 Amplification Mediates Resistance to Gefitinib in Glioblastoma Cells'. *Oncotarget* 6 (24): 20388–95.

Ambrogio, Chiara, Gonzalo Gómez-López, Mattia Falcone, August Vidal, Ernest Nadal, Nicola Crosetto, Rafael B. Blasco, et al. 2016. 'Combined Inhibition of DDR1 and Notch Signaling Is a Therapeutic Strategy for KRAS-Driven Lung Adenocarcinoma'. *Nature Medicine* 22 (3): 270–77. https://doi.org/10.1038/nm.4041.

Ascierto, Paolo A., John M. Kirkwood, Jean-Jacques Grob, Ester Simeone, Antonio M. Grimaldi, Michele Maio, Giuseppe Palmieri, Alessandro Testori, Francesco M. Marincola, and Nicola Mozzillo. 2012. 'The Role of BRAF V600 Mutation in Melanoma'. *Journal of Translational Medicine* 10 (July): 85. https://doi.org/10.1186/1479-5876-10-85.

Badiola, Iker, Patricia Villacé, Iratxe Basaldua, and Elvira Olaso. 2011. 'Downregulation of Discoidin Domain Receptor 2 in A375 Human Melanoma Cells Reduces Its Experimental Liver Metastasis Ability'. *Oncology Reports* 26 (4): 971–78. https://doi.org/10.3892/or.2011.1356.

Basile, Kevin J., Kaitlyn Le, Edward J. Hartsough, and Andrew E. Aplin. 2014. 'Inhibition of Mutant BRAF Splice Variant Signaling by Next-Generation, Selective RAF Inhibitors'. *Pigment Cell & Melanoma Research* 27 (3): 479–84. https://doi.org/10.1111/pcmr.12218.

Bray, Freddie, Jacques Ferlay, Isabelle Soerjomataram, Rebecca L. Siegel, Lindsey A. Torre, and Ahmedin Jemal. 2018. 'Global Cancer Statistics 2018: GLOBOCAN Estimates of Incidence and Mortality Worldwide for 36 Cancers in 185 Countries'. *CA: A Cancer Journal for Clinicians* 68 (6): 394–424. https://doi.org/10.3322/caac.21492.

Chapman, Paul B., Axel Hauschild, Caroline Robert, John B. Haanen, Paolo Ascierto, James Larkin, Reinhard Dummer, et al. 2011. 'Improved Survival with Vemurafenib in Melanoma with BRAF V600E Mutation'. *The New England Journal of Medicine* 364 (26): 2507–16. https://doi.org/10.1056/NEJMoa1103782.

Chetoui, Nizar, Mohammed-Amine El Azreq, Marc Boisvert, Marie-Ève Bergeron, and Fawzi Aoudjit. 2011. 'Discoidin Domain Receptor 1 Expression in Activated T Cells Is Regulated by the ERK MAP Kinase Signaling Pathway'. *Journal of Cellular Biochemistry* 112 (12): 3666–74. https://doi.org/10.1002/jcb.23300.

Conde-Perez, Alejandro, and Lionel Larue. 2014. 'Human Relevance of NRAS/BRAF Mouse Melanoma Models'. *European Journal of Cell Biology* 93 (1–2): 82–86. https://doi.org/10.1016/j.ejcb.2013.10.010.

Corsa, Callie A. S., Audrey Brenot, Whitney R. Grither, Samantha Van Hove, Andrew J. Loza, Kun Zhang, Suzanne M. Ponik, et al. 2016. 'The Action of Discoidin Domain Receptor 2 in Basal Tumor Cells and Stromal Cancer Associated Fibroblasts Is Critical for Breast Cancer Metastasis'. *Cell Reports* 15 (11): 2510–23. https://doi.org/10.1016/j.celrep.2016.05.033.

Das, Sanjeev, Pat P. Ongusaha, Yoon Sun Yang, Jin-Mo Park, Stuart A. Aaronson, and Sam W. Lee. 2006a. 'Discoidin Domain Receptor 1 Receptor Tyrosine Kinase Induces Cyclooxygenase-2 and Promotes Chemoresistance through Nuclear Factor-KappaB Pathway Activation'. *Cancer Research* 66 (16): 8123–30. https://doi.org/10.1158/0008-5472.CAN-06-1215. 2006b. 'Discoidin Domain Receptor 1 Receptor Tyrosine Kinase Induces Cyclooxygenase-2 and Promotes Chemoresistance through Nuclear Factor-KappaB Pathway Activation'. *Cancer Research* 66 (16): 8123–30. https://doi.org/10.1158/0008-5472.CAN-06-1215.

Davies, Helen, Graham R. Bignell, Charles Cox, Philip Stephens, Sarah Edkins, Sheila Clegg, Jon Teague, et al. 2002. 'Mutations of the BRAF Gene in Human Cancer'. *Nature* 417 (6892): 949–54. https://doi.org/10.1038/nature00766.

Day, Elizabeth, Beatrice Waters, Katrin Spiegel, Tanja Alnadaf, Paul W. Manley, Elisabeth Buchdunger, Christoph Walker, and Gabor Jarai. 2008. 'Inhibition of Collagen-Induced Discoidin Domain Receptor 1 and 2 Activation by Imatinib, Nilotinib and Dasatinib'. *European Journal of Pharmacology* 599 (1–3): 44–53. https://doi.org/10.1016/j.ejphar.2008.10.014.

Deng, Yuao, Fang Zhao, Liu Hui, Xiuyun Li, Danyu Zhang, Wang Lin, Zhiqiang Chen, and Yingxia Ning. 2017a. 'Suppressing MiR-199a-3p by Promoter Methylation Contributes to Tumor Aggressiveness and Cisplatin Resistance of Ovarian Cancer through Promoting DDR1 Expression'. *Journal of Ovarian Research* 10 (1): 50. https://doi.org/10.1186/s13048-017-0333-4.2017b. 'Suppressing MiR-199a-3p by Promoter Methylation Contributes to Tumor Aggressiveness and Cisplatin Resistance of Ovarian Cancer through Promoting DDR1 Expression'. *Journal of Ovarian Research* 10 (July). https://doi.org/10.1186/s13048-017-0333-4.

Du, Zhenfang, and Christine M. Lovly. 2018. 'Mechanisms of Receptor Tyrosine Kinase Activation in Cancer'. *Molecular Cancer* 17 (1): 58. https://doi.org/10.1186/s12943-018-0782-4.

Duncan, James S., Martin C. Whittle, Kazuhiro Nakamura, Amy N. Abell, Alicia A. Midland, Jon S. Zawistowski, Nancy L. Johnson, et al. 2012. 'Dynamic Reprogramming of the Kinome in Response to Targeted MEK Inhibition in Triple-Negative Breast Cancer'. *Cell* 149 (2): 307–21. https://doi.org/10.1016/j.cell.2012.02.053.

El Azreq, Mohammed-Amine, Maleck Kadiri, Marc Boisvert, Nathalie Pagé, Philippe A. Tessier, and Fawzi Aoudjit. 2016. 'Discoidin Domain Receptor 1 Promotes Th17 Cell Migration by Activating the RhoA/ROCK/MAPK/ERK Signaling Pathway'. *Oncotarget* 7 (29): 44975–90. https://doi.org/10.18632/oncotarget.10455.

Elder, David E., D. Massi, Rein Willemze, and R. Scolyer. 2018. *WHO Classification of Skin Tumours*. International Agency for Research on Cancer.

Ezzoukhry, Zakaria, Elodie Henriet, Léo Piquet, Kevin Boyé, Paulette Bioulac-Sage, Charles Balabaud, Gabrielle Couchy, Jessica Zucman-Rossi, Violaine Moreau, and Frédéric Saltel. 2016. 'TGF-B1 Promotes Linear Invadosome Formation in Hepatocellular Carcinoma Cells, through DDR1 up-Regulation and Collagen I Cross-Linking'. *European Journal of Cell Biology* 95 (11): 503–12. https://doi.org/10.1016/j.ejcb.2016.09.003.

Flaherty, Keith T., Caroline Robert, Peter Hersey, Paul Nathan, Claus Garbe, Mohammed Milhem, Lev V. Demidov, et al. 2012. 'Improved Survival with MEK Inhibition in BRAF-Mutated Melanoma'. *The New England Journal of Medicine* 367 (2): 107–14. https://doi.org/10.1056/NEJMoa1203421.

Gao, Mingshan, Lei Duan, Jinfeng Luo, Lianwen Zhang, Xiaoyun Lu, Yan Zhang, Zhang Zhang, et al. 2013. 'Discovery and Optimization of 3-(2-(Pyrazolo[1,5-a]Pyrimidin-6-Yl)Ethynyl)Benzamides as Novel Selective and Orally Bioavailable Discoidin Domain Receptor 1 (DDR1) Inhibitors'. *Journal of Medicinal Chemistry* 56 (8): 3281–95. https://doi.org/10.1021/jm301824k.

Gonzalez, Maria E., Emily E. Martin, Talha Anwar, Caroline Arellano-Garcia, Natasha Medhora, Arjun Lama, Yu-Chih Chen, et al. 2017. 'Mesenchymal Stem Cell-Induced DDR2 Mediates Stromal-Breast Cancer Interactions and Metastasis Growth'. *Cell Reports* 18 (5): 1215–28. https://doi.org/10.1016/j.celrep.2016.12.079.

Grither, Whitney R., and Gregory D. Longmore. 2018. 'Inhibition of Tumor–Microenvironment Interaction and Tumor Invasion by Small-Molecule Allosteric Inhibitor of DDR2 Extracellular Domain'. *Proceedings of the National Academy of Sciences of the United States of America* 115 (33): E7786–94. https://doi.org/10.1073/pnas.1805020115.

Hammerman, Peter S., Martin L. Sos, Alex H. Ramos, Chunxiao Xu, Amit Dutt, Wenjun Zhou, Lear E. Brace, et al. 2011. 'Mutations in the DDR2 Kinase Gene Identify a Novel Therapeutic Target in Squamous Cell Lung Cancer'. *Cancer Discovery* 1 (1): 78–89. https://doi.org/10.1158/2159-8274.CD-11-0005.

Hauschild, Axel, Jean-Jacques Grob, Lev V. Demidov, Thomas Jouary, Ralf Gutzmer, Michael Millward, Piotr Rutkowski, et al. 2012. 'Dabrafenib in BRAF-Mutated Metastatic Melanoma: A Multicentre, Open-Label, Phase 3 Randomised Controlled Trial'. *The Lancet* 380 (9839): 358–65. https://doi.org/10.1016/S0140-6736(12)60868-X.

Hedberg, Matthew L., Gerald Goh, Simion I. Chiosea, Julie E. Bauman, Maria L. Freilino, Yan Zeng, Lin Wang, et al. 2016. 'Genetic Landscape of Metastatic and Recurrent Head and Neck Squamous Cell Carcinoma'. *The Journal of Clinical Investigation* 126 (1): 169–80. https://doi.org/10.1172/JCI82066.

Henriet, Elodie, Aya Abou Hammoud, Jean-William Dupuy, Benjamin Dartigues, Zakaria Ezzoukry, Nathalie Dugot-Senant, Thierry Leste-Lasserre, et al. 2017. 'Argininosuccinate Synthase 1 (ASS1): A Marker of Unclassified Hepatocellular Adenoma and High Bleeding Risk'. *Hepatology* 66 (6): 2016–28. https://doi.org/10.1002/hep.29336.

Henriet, Elodie, Margaux Sala, Aya Abou Hammoud, Adjanie Tuariihionoa, Julie Di Martino, Manon Ros, and Frédéric Saltel. 2018. 'Multitasking Discoidin Domain Receptors Are Involved in Several and Specific Hallmarks of Cancer'. *Cell Adhesion & Migration* 12 (4):

363–77. https://doi.org/10.1080/19336918.2018.1465156.

Hidalgo-Carcedo, Cristina, Steven Hooper, Shahid I. Chaudhry, Peter Williamson, Kevin Harrington, Birgit Leitinger, and Erik Sahai. 2011. 'Collective Cell Migration Requires Suppression of Actomyosin at Cell-Cell Contacts Mediated by DDR1 and the Cell Polarity Regulators Par3 and Par6'. *Nature Cell Biology* 13 (1): 49–58. https://doi.org/10.1038/ncb2133.

Jin, Hyejin, In-Hye Ham, Hye Jeong Oh, Cheong A. Bae, Dakeun Lee, Young-Bae Kim, Sang-Yong Son, et al. 2018. 'Inhibition of Discoidin Domain Receptor 1 Prevents Stroma-Induced Peritoneal Metastasis in Gastric Carcinoma'. *Molecular Cancer Research* 16 (10): 1590–1600. https://doi.org/10.1158/1541-7786.MCR-17-0710.

Juin, Amélie, Julie Di Martino, Birgit Leitinger, Elodie Henriet, Anne-Sophie Gary, Lisa Paysan, Jeremy Bomo, et al. 2014. 'Discoidin Domain Receptor 1 Controls Linear Invadosome Formation via a Cdc42-Tuba Pathway'. *The Journal of Cell Biology* 207 (4): 517–33. https://doi.org/10.1083/jcb.201404079.

Keating, Gillian M. 2017. 'Dasatinib: A Review in Chronic Myeloid Leukaemia and Ph+ Acute Lymphoblastic Leukaemia'. *Drugs* 77 (1): 85–96. https://doi.org/10.1007/s40265-016-0677-x.

Kim, Hyung-Gu, Li Tan, Ellen L. Weisberg, Feiyang Liu, Peter Canning, Hwan Geun Choi, Scott A. Ezell, et al. 2013. 'Discovery of a Potent and Selective DDR1 Receptor Tyrosine Kinase Inhibitor'. *ACS Chemical Biology* 8 (10): 2145–50. https://doi.org/10.1021/cb400430t.

Kurashige, Junji, Takanori Hasegawa, Atsushi Niida, Keishi Sugimachi, Niantao Deng, Kosuke Mima, Ryutaro Uchi, et al. 2016. 'Integrated Molecular Profiling of Human Gastric Cancer Identifies DDR2 as a Potential Regulator of Peritoneal Dissemination'. *Scientific Reports* 6 (March): 22371. https://doi.org/10.1038/srep22371.

Larkin, James M. G., Yibing Yan, Grant A. McArthur, Paolo Antonio Ascierto, Gabriella Liszkay, Michele Maio, Mario Mandalà, et al. 2015. 'Update of Progression-Free Survival (PFS) and Correlative Biomarker Analysis from CoBRIM: Phase III Study of Cobimetinib (Cobi) plus Vemurafenib (Vem) in Advanced BRAF-Mutated Melanoma.' *Journal of Clinical Oncology* 33 (15_suppl): 9006–9006. https://doi.org/10.1200/jco.2015.33.15_suppl.9006.

Leitinger, Birgit. 2003. 'Molecular Analysis of Collagen Binding by the Human Discoidin Domain Receptors, DDR1 and DDR2 IDENTIFICATION OF COLLAGEN BINDING SITES IN DDR2'. *Journal of Biological Chemistry* 278 (19): 16761–69. https://doi.org/10.1074/jbc.M301370200.
. 2014. 'Discoidin Domain Receptor Functions in Physiological and Pathological Conditions'. *International Review of Cell and Molecular Biology* 310: 39–87. https://doi.org/10.1016/B978-0-12-800180-6.00002-5.

Leitinger, Birgit, and Alvin P. L. Kwan. 2006. 'The Discoidin Domain Receptor DDR2 Is a Receptor for Type X Collagen'. *Matrix Biology* 25 (6): 355–64. https://doi.org/10.1016/j.matbio.2006.05.006.

Long, Georgina V, Daniil Stroyakovskiy, Helen Gogas, Evgeny Levchenko, Filippo de Braud,

James Larkin, Claus Garbe, et al. 2015. 'Dabrafenib and Trametinib versus Dabrafenib and Placebo for Val600 BRAF-Mutant Melanoma: A Multicentre, Double-Blind, Phase 3 Randomised Controlled Trial'. *The Lancet* 386 (9992): 444–51. https://doi.org/10.1016/S0140-6736(15)60898-4.

Lu, Qiu-Ping, Wen-Dan Chen, Jie-Ren Peng, Yao-Dong Xu, Qian Cai, Gong-Kan Feng, Ke Ding, Xiao-Feng Zhu, and Zhong Guan. 2016. 'Antitumor Activity of 7RH, a Discoidin Domain Receptor 1 Inhibitor, Alone or in Combination with Dasatinib Exhibits Antitumor Effects in Nasopharyngeal Carcinoma Cells'. *Oncology Letters* 12 (5): 3598–3608. https://doi.org/10.3892/ol.2016.5088.

Luke, Jason J., Keith T. Flaherty, Antoni Ribas, and Georgina V. Long. 2017. 'Targeted Agents and Immunotherapies: Optimizing Outcomes in Melanoma'. *Nature Reviews. Clinical Oncology* 14 (8): 463–82. https://doi.org/10.1038/nrclinonc.2017.43.

Malaguarnera, Roberta, Maria Luisa Nicolosi, Antonella Sacco, Alaide Morcavallo, Veronica Vella, Concetta Voci, Michela Spatuzza, et al. 2015. 'Novel Cross Talk between IGF-IR and DDR1 Regulates IGF-IR Trafficking, Signaling and Biological Responses'. *Oncotarget* 6 (18): 16084–105. https://doi.org/10.18632/oncotarget.3177.

Misek, S. A., K. M. Appleton, T. S. Dexheimer, E. M. Lisabeth, R. S. Lo, S. D. Larsen, K. A. Gallo, and R. R. Neubig. 2019. 'Rho-Mediated Signaling Promotes BRAF Inhibitor Resistance in de-Differentiated Melanoma Cells'. *Oncogene*, October. https://doi.org/10.1038/s41388-019-1074-1.

Nazarian, Ramin, Hubing Shi, Qi Wang, Xiangju Kong, Richard C. Koya, Hane Lee, Zugen Chen, et al. 2010. 'Melanomas Acquire Resistance to B-RAF(V600E) Inhibition by RTK or N-RAS Upregulation'. *Nature* 468 (7326): 973–77. https://doi.org/10.1038/nature09626.

Nemoto, T., K. Ohashi, T. Akashi, J. D. Johnson, and K. Hirokawa. 1997. 'Overexpression of Protein Tyrosine Kinases in Human Esophageal Cancer'. *Pathobiology: Journal of Immunopathology, Molecular and Cellular Biology* 65 (4): 195–203. https://doi.org/10.1159/000164123.

Ongusaha, Pat P., Jong-il Kim, Li Fang, Tai W. Wong, George D. Yancopoulos, Stuart A. Aaronson, and Sam W. Lee. 2003. 'P53 Induction and Activation of DDR1 Kinase Counteract P53-Mediated Apoptosis and Influence P53 Regulation through a Positive Feedback Loop'. *The EMBO Journal* 22 (6): 1289–1301. https://doi.org/10.1093/emboj/cdg129.

Park, Joong-Won, Yeon-Su Lee, Jin Sook Kim, Sook-Kyung Lee, Bo Hyun Kim, Jung Ahn Lee, Nam Oak Lee, Seong Hoon Kim, and Eun Kyung Hong. 2015. 'Downregulation of Discoidin Domain Receptor 2 Decreases Tumor Growth of Hepatocellular Carcinoma'. *Journal of Cancer Research and Clinical Oncology* 141 (11): 1973–83. https://doi.org/10.1007/s00432-015-1967-5.

Payne, Leo S., and Paul H. Huang. 2014. 'Discoidin Domain Receptor 2 Signaling Networks and Therapy in Lung Cancer'. *Journal of Thoracic Oncology: Official Publication of the International Association for the Study of Lung Cancer* 9 (6): 900–904. https://doi.org/10.1097/JTO.0000000000000164.

Pitini, Vincenzo, Carmela Arrigo, Cristian Di Mirto, Patrizia Mondello, and Giuseppe

Altavilla. 2013. 'Response to Dasatinib in a Patient with SQCC of the Lung Harboring a Discoid-Receptor-2 and Synchronous Chronic Myelogenous Leukemia'. *Lung Cancer (Amsterdam, Netherlands)* 82 (1): 171–72. https://doi.org/10.1016/j.lungcan.2013.07.004.

Poudel, Barun, Young-Mi Lee, and Dae-Ki Kim. 2015. 'DDR2 Inhibition Reduces Migration and Invasion of Murine Metastatic Melanoma Cells by Suppressing MMP2/9 Expression through ERK/NF-KB Pathway'. *Acta Biochimica et Biophysica Sinica* 47 (4): 292–98. https://doi.org/10.1093/abbs/gmv005.

Rada, Miran, Sameera Nallanthighal, Jennifer Cha, Kerry Ryan, Jessica Sage, Catherine Eldred, Maria Ullo, Sandra Orsulic, and Dong-Joo Cheon. 2018. 'Inhibitor of Apoptosis Proteins (IAPs) Mediate Collagen Type XI Alpha 1-Driven Cisplatin Resistance in Ovarian Cancer'. *Oncogene* 37 (35): 4809–20. https://doi.org/10.1038/s41388-018-0297-x.

Rammal, Hassan, Charles Saby, Kevin Magnien, Laurence Van-Gulick, Roselyne Garnotel, Emilie Buache, Hassan El Btaouri, Pierre Jeannesson, and Hamid Morjani. 2016. 'Discoidin Domain Receptors: Potential Actors and Targets in Cancer'. *Frontiers in Pharmacology* 7 (March). https://doi.org/10.3389/fphar.2016.00055.

Reger de Moura, Coralie, Maxime Battistella, Anjum Sohail, Anne Caudron, Jean Paul Feugeas, Marie-Pierre Podgorniak, Cecile Pages, et al. 2019. 'Discoidin Domain Receptors: A Promising Target in Melanoma'. *Pigment Cell & Melanoma Research* 32 (5): 697–707. https://doi.org/10.1111/pcmr.12809.

Ren, Tingting, Jian Zhang, Jing Zhang, Xinping Liu, and Libo Yao. 2013. 'Increased Expression of Discoidin Domain Receptor 2 (DDR2): A Novel Independent Prognostic Marker of Worse Outcome in Breast Cancer Patients'. *Medical Oncology (Northwood, London, England)* 30 (1): 397. https://doi.org/10.1007/s12032-012-0397-3.

Ren, Tingting, Wei Zhang, Xinping Liu, Hu Zhao, Jian Zhang, Jing Zhang, Xia Li, et al. 2014. 'Discoidin Domain Receptor 2 (DDR2) Promotes Breast Cancer Cell Metastasis and the Mechanism Implicates Epithelial-Mesenchymal Transition Programme under Hypoxia'. *The Journal of Pathology* 234 (4): 526–37. https://doi.org/10.1002/path.4415.

Rudra-Ganguly, Nandini, Christine Lowe, Michael Mattie, Mi Sook Chang, Daulet Satpayev, Alla Verlinsky, Zili An, et al. 2014. 'Discoidin Domain Receptor 1 Contributes to Tumorigenesis through Modulation of TGFBI Expression'. *PloS One* 9 (11): e111515. https://doi.org/10.1371/journal.pone.0111515.

Sekiya, Yumiko, Tomohiro Ogawa, Katsutoshi Yoshizato, Kazuo Ikeda, and Norifumi Kawada. 2011. 'Suppression of Hepatic Stellate Cell Activation by MicroRNA-29b'. *Biochemical and Biophysical Research Communications* 412 (1): 74–79. https://doi.org/10.1016/j.bbrc.2011.07.041.

Shrivastava, Ajay, Czeslaw Radziejewski, Ernest Campbell, Lubomir Kovac, Marion McGlynn, Terence E. Ryan, Sam Davis, et al. 1997. 'An Orphan Receptor Tyrosine Kinase Family Whose Members Serve as Nonintegrin Collagen Receptors'. *Molecular Cell* 1 (1): 25–34. https://doi.org/10.1016/S1097-2765(00)80004-0.

Søndergaard, Jonas N, Ramin Nazarian, Qi Wang, Deliang Guo, Teli Hsueh, Stephen Mok, Hooman Sazegar, et al. 2010. 'Differential Sensitivity of Melanoma Cell Lines with

BRAFV600E Mutation to the Specific Raf Inhibitor PLX4032'. *Journal of Translational Medicine* 8 (April): 39. https://doi.org/10.1186/1479-5876-8-39.

Sullivan, Ryan J., and Keith T. Flaherty. 2013. 'Resistance to BRAF-Targeted Therapy in Melanoma'. *European Journal of Cancer (Oxford, England: 1990)* 49 (6): 1297–1304. https://doi.org/10.1016/j.ejca.2012.11.019.

Valiathan, Rajeshwari R., Marta Marco, Birgit Leitinger, Celina G. Kleer, and Rafael Fridman. 2012a. 'Discoidin Domain Receptor Tyrosine Kinases: New Players in Cancer Progression'. *Cancer Metastasis Reviews* 31 (1–2): 295–321. https://doi.org/10.1007/s10555-012-9346-z.
2012b. 'Discoidin Domain Receptor Tyrosine Kinases: New Players in Cancer Progression'. *Cancer Metastasis Reviews* 31 (1–2): 295–321. https://doi.org/10.1007/s10555-012-9346-z.

Villanueva, Jessie, Adina Vultur, John T. Lee, Rajasekharan Somasundaram, Mizuho Fukunaga-Kalabis, Angela K. Cipolla, Bradley Wubbenhorst, et al. 2010. 'Acquired Resistance to BRAF Inhibitors Mediated by a RAF Kinase Switch in Melanoma Can Be Overcome by Cotargeting MEK and IGF-1R/PI3K'. *Cancer Cell* 18 (6): 683–95. https://doi.org/10.1016/j.ccr.2010.11.023.

Vogel, Wolfgang, Gerald D. Gish, Frauke Alves, and Tony Pawson. 1997. 'The Discoidin Domain Receptor Tyrosine Kinases Are Activated by Collagen'. *Molecular Cell* 1 (1): 13–23. https://doi.org/10.1016/S1097-2765(00)80003-9.

Wagenaar, Timothy R., Leyuan Ma, Benjamin Roscoe, Sung Mi Park, Daniel N. Bolon, and Michael R. Green. 2014. 'Resistance to Vemurafenib Resulting from a Novel Mutation in the BRAFV600E Kinase Domain'. *Pigment Cell & Melanoma Research* 27 (1): 124–33. https://doi.org/10.1111/pcmr.12171.

Wang, Liqin, Rodrigo Leite de Oliveira, Sanne Huijberts, Evert Bosdriesz, Nora Pencheva, Diede Brunen, Astrid Bosma, et al. 2018. 'An Acquired Vulnerability of Drug-Resistant Melanoma with Therapeutic Potential'. *Cell* 173 (6): 1413-1425.e14. https://doi.org/10.1016/j.cell.2018.04.012.

Xiao, Qian, Yan Jiang, Qingbo Liu, Jiao Yue, Chunying Liu, Xiaotong Zhao, Yuemei Qiao, Hongbin Ji, Jianfeng Chen, and Gaoxiang Ge. 2015. 'Minor Type IV Collagen A5 Chain Promotes Cancer Progression through Discoidin Domain Receptor-1'. *PLoS Genetics* 11 (5): e1005249. https://doi.org/10.1371/journal.pgen.1005249.

Figures Legends

Figure 1: DDRs expression in resistant cell lines as compared to the sensitive
A) Western blotting analysis of P Erk and Erk expression in a subset of two melanoma cell lines (229 and 238) sensitive (S) or resistant (R) to vemurafenib. GAPDH was used as the endogenous loading control. The graph shows the quantification of Perk/Erk expression. Values are expressed as the mean ± SEM of three independent experiments. The differential expression between the different conditions was validated by a paired t test *P<0.05, **P<0.01. B) mRNA level of DDR1 and DDR2 in a subset of two melanoma cell lines (229 and 238) sensitive (S) or resistant (R) to vemurafenib. The graph shows the quantification of DDRs mRNA level. Values are expressed as the mean ± SEM of three independent experiments. The differential expression between the different conditions was validated by a paired t test *P<0.05. C) Western blotting analysis of DDR1 and DDR2 expression in a subset of two melanoma cell lines (229 and 238) sensitive (S) or resistant (R) to vemurafenib. GAPDH was used as the endogenous loading control. The graph shows the quantification of DDRs expression. Values are expressed as the mean ± SEM of three independent experiments. The differential expression between the cell lines was validated by a t test *P<0.05. D) Western blotting analysis of DDR1 and DDR2 expression in a 229 sensitives cell lines treated with vemurafenib (10 nM), cobimetinib (10 nM) or both during 2 months. GAPDH was used as the endogenous loading control.

Figure 2: DDRs role in MAP kinase pathway.
A) 238R (left panel) cells were transfected with a siRNA control (siGl2) or targeting DDR1 (siDDR1), DDR2 (siDDR2) or both (siDDR1&2). Protein extracts were then analyzed by immunoblotting to determine PErk and Erk expression. GAPDH was used as the endogenous loading control. The graph shows the quantification of PErk/Erk expression. Values are expressed as the mean ± SEM of three independent experiments. The differential expression between the control and the different conditions was validated by a paired t test *P<0.05, **P<0.01. **B**) mRNA level of MAP kinase targets in 238 resistant (R) to vemurafenib. The graph shows the quantification of PHLDA1, SPRY2, DUSP6, DUSP4, ETV4, ETV5 mRNA level. Values are expressed as the mean ± SEM of three independent experiments. The differential expression between the control and the different conditions was validated by a paired t test *P<0.05, ***P<0.001. **C**) 238R were treated with dasatinib during 2 hours. Protein extract were then analyzed by immunoblotting to determine PErk, Erk, DDR1 and DDDR2 expression. GAPDH was used as the endogenous loading control. The graph shows the quantification of the ratio of PDDR1/DDR1, PDDR2/DDR2 and PErk/Erk. Values are expressed as the mean ± SEM of three independent experiments. The differential expression between the conditions was validated by a paired t test **P<0.01.

Figure 3: DDRs role in proliferation
A) Incucyte proliferation assay of 238R cells seeded at 5 000 cells per well in a 96 well plate. The cells were transfected with a siRNA control (siGl2) or targeting DDR1 (siDDR1), DDR2 (siDDR2) or both (siDDR1&2). The differential proliferation between the control and the different conditions was validated by a paired t test *P<0.05. B) Incucyte proliferation assay of 238R cells seeded at 5 000 cells per well in a 96 well plate cultured in the presence or absence of 100 nM dasatinib. The differential proliferation between the control and the different conditions was validated by a paired t test **P<0.01. C) Proliferation of 229 R cells seeded at 5 000 cells per well in a 96 well plate. The cells were transfected with DDR2 WT-myc or DDR2 KD(K608E)-myc. The differential proliferation between the control and

different conditions was validated by a paired t test *P<0.05. Protein extracts were then analyzed by immunoblotting to determine DDR2-myc expression. GAPDH was used as the endogenous loading control. D) Incucyte proliferation assay of 229R cells seeded at 5 000 cells per well in a 96 well plate cultured in the presence or absence of DDR2 inhibitor. The differential proliferation between the control and different conditions was validated by a paired t test *P<0.05, **P<0.01, ***P<0.001. Protein extracts were then analyzed by immunoblotting to determine P DDR2, DDR2, P Erk, Erk expression. GAPDH was used as the endogenous loading control. The graph shows the quantification of the ratio of PDDR2/DDR2 and PErk/Erk. Values are expressed as the mean ± SEM of three independent experiments. The differential expression between the conditions was validated by a paired t test ***P<0.001.

Figure 4: DDRs role in spheroid maintenance

A) 238 R cells were seeded to form spheroids and spheroid at 72 hours were treated with Dasatinib at 100 nM. B) The graph shows the quantification of the area in the different conditions. Values are expressed as the mean ± SEM of three independent experiments. The differential area quantification was validated by a paired t test *P<0.05. C) Incucyte apoptotic assay of 238R cells seeded at 5 000 cells per well in a 96 well plate cultured in the presence or absence of dasatinib (100 nM). The differential proliferation between the different conditions was validated by a paired t test *P<0.05. D) The Spheroids at 72 hours were treated with DDR2 inhibitor at 5 µM. E) The graph shows the quantification of the area in the different conditions. Values are expressed as the mean ± SEM of three independent experiments. The differential area was validated by a paired t test **P<0.01. F) Incucyte apoptotic assay of 229R cells seeded at 5 000 cells per well in a 96 well plate cultured in the presence or absence of DDR2 inhibitor (5 µM). The differential proliferation between the different conditions was validated by a paired t test **P<0.01.

Figure 5: DDRs role *in vivo*

A) 229 R cells ($5*10^6$ cells) were implanted subcutaneously into the left flank of the mouse. When the tumor reached 150 mm^3, the mice were randomly assigned in 2 groups: one control group where the mice are treated with Vemurafenib (40 mg/kg), and the other group where the mice are treated with dasatinib (20 mg/kg) (n=5 in each condition). **B**) Tumor growth of 229 R in the left flank of NOG mice subcutaneously injected with $5*10^6$ 228R cells. **C**) Photographs of mice treated with vemurafenib or dasatinib. **D**) Western blotting analysis of DDR1 DDR2, PDDR1, PDDR2 expression in mouse primary tumor treated or not with dasatinib. GAPDH was used as the endogenous loading control. The graph shows the quantification of the ratio of PDDR1/DDR1, PDDR2/DDR2. **E**) Immunohistochemistry of mouse primary tumor treated or not with dasatinib. Left panel: HES of mouse primary tumor. Right panel: Immunostaining of Annexin V. **F**) RNA sequencing data for DDR1 or DDR2 abundance after treatment to an anti-BRAF. All the dots above the black lines, meaning that there is an increase of receptor's abundance after treatment (in grey if DDR1 is overexpressed, in blue if DDR2 is overexpressed, in red if DDR1 and 2 are overexpressed).

Supplementary figure 1: DDRs role in MAP kinase pathway.

A) 229R cells were transfected with a siRNA control (siGl2) or targeting DDR1 (siDDR1), DDR2 (siDDR2) or both (siDDR1&2). Protein extracts were then analyzed by immunoblotting to determine PErk and Erk expression. GAPDH was used as the endogenous loading control. **B**) mRNA level of MAP kinase targets in 229 resistant (R) to vemurafenib. The graph shows the quantification of PHLDA1, SPRY2, DUSP6, DUSP4, ETV4, ETV5 expression. Values are expressed as the mean ± SEM of three independent experiments. The

differential mRNA level between the control and different conditions was validated by a paired t test *P<0.05. **C**) 229R were treated with dasatinib during 2 hours. Protein extract were then analyzed by immunoblotting to determine PErk and Erk expression. GAPDH was used as the endogenous loading control. The graph shows the quantification of the ratio of PDDR1/DDR1, PDDR2/DDR2 and PErk/Erk. Values are expressed as the mean ± SEM of three independent experiments. The differential expression between the conditions was validated by a paired t test *P<0.05, **P<0.01.

Supplementary figure 2: DDRs role in proliferation

A) Incucyte proliferation assay of 229 R cells seeded at 5 000 cells per well in a 96 well plate. The cells were transfected with a siRNA control (sGl2) or targeting DDR1 (siDDR1), DDR2 (siDDR2) or both (siDDR1&2). The differential proliferation between the different conditions was validated by a paired t test *P<0.05. **B**) Incucyte proliferation assay of 229R cells seeded at 5 000 cells per well in a 96 well plate cultured in the presence or absence of 100 nM dasatinib. The differential proliferation between the control and the different conditions was validated by a paired t test **P<0.01. **C**) Proliferation of 238R cells seeded at 5 000 cells per well in a 96 well plate. The cells were transfected with DDR2 WT-myc or DDR2 KD(K608E)-myc. The differential proliferation between the control and the different conditions was validated by one-way ANOVA *P<0.05. **D**) Incucyte proliferation assay of 238R cells seeded at 5 000 cells per well in a 96 well plate cultured in the presence or absence of DDR2 inhibitor. The differential proliferation between the control and the different conditions was validated by a one-way ANOVA *P<0.05. **E**) 238R were transfected with a siRNA control (siCtrl) or targeting DDR2 (siDDR2) or treated with DDR2 inhibitor during 72 hours. 238R cells were treated with dasatinib during 2 hours. Protein extract were then analyzed by immunoblotting to determine PErk, Erk, PAkt and Akt expression. Protein extracts were analyzed by immunoblotting to determine P DDR2, DDR2, P Src, Src expression. GAPDH was used as the endogenous loading control. The graph shows the quantification of the ratio of PSrc/Src. Values are expressed as the mean ± SEM of three independent experiments. The differential expression between the conditions was validated by a one-way ANOVA or a paired t test: ns: non-significant.

Supplementary figure 3: GSEA analysis

Pathways commonly and significantly enriched between the following conditions: 238R cells treated with dasatinib, with a DDR inhibitor or transfected with siRNA targeting DDR2. Gene set enrichment analysis (GSEA) was performed against the Ingenuity Pathways database (fisher test expressed in -log10pvalue).

Supplementary figure 4: DDRs role in spheroid maintenance in 229R

A) 229 R cells were seeded to form spheroids and spheroid at 72 h were treated with dasatinib at 100 nM. B) The graph shows the quantification of the area in the different conditions. Values are expressed as the mean ± SEM of three independent experiments. The differential expression was validated by a paired t test ***P<0.001. C) Incucyte apoptotic assay of 229R cells seeded at 5 000 cells per well in a 96 well plate cultured in the presence or absence of dasatinib (100 nM). The differential proliferation between the different conditions was validated by a paired t test *P<0.05.

Supplementary table 1: List of PCR primers

Figure 1: DDRs expression in resistant cell lines as compared to the sensitive

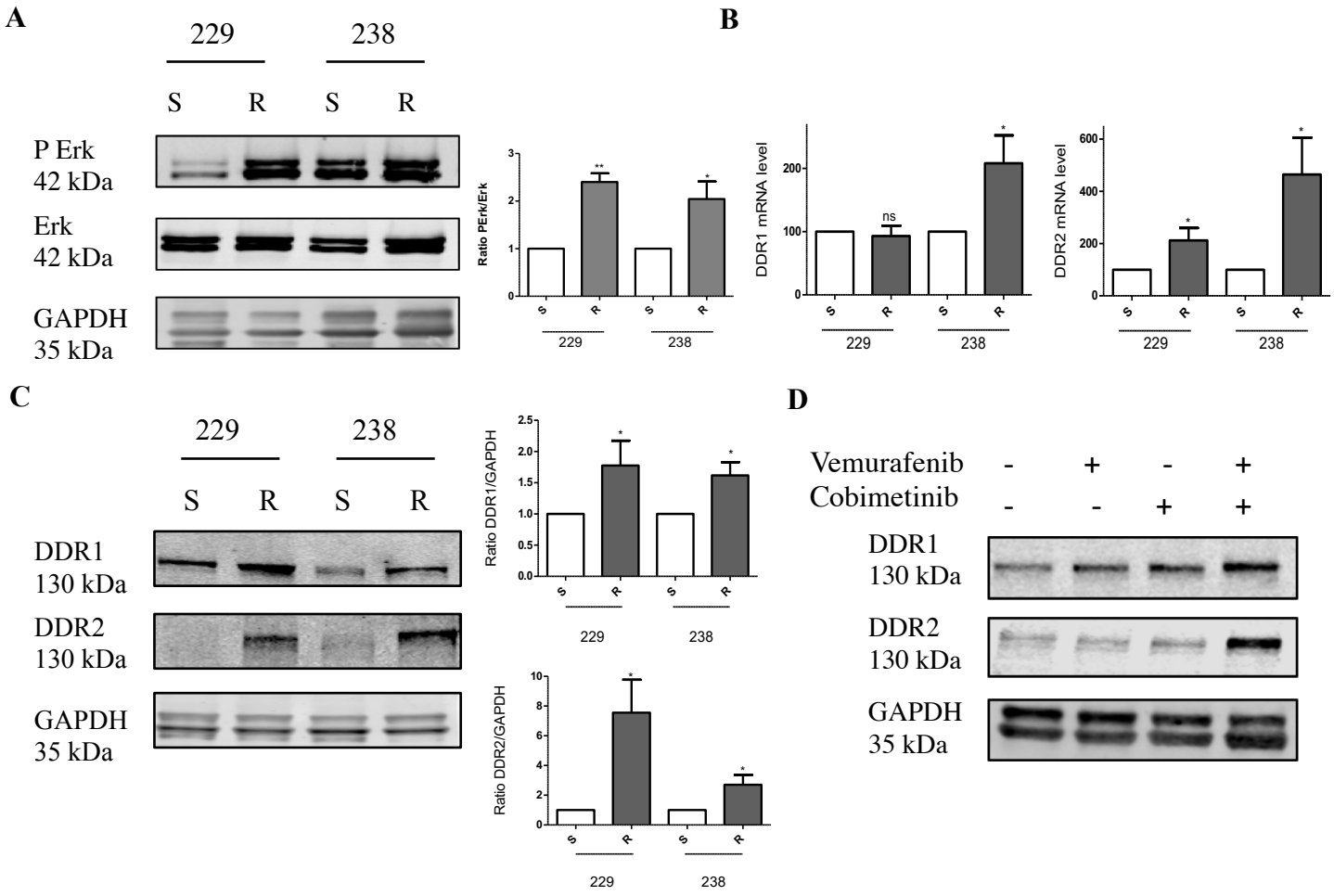

Figure 1: DDRs expression in resistant cell lines as compared to the sensitive

A) Western blotting analysis of P Erk and Erk expression in a subset of two melanoma cell lines (229 and 238) sensitive (S) or resistant (R) to Vemurafenib. GAPDH was used as the endogenous loading control. The graph shows the quantification of Perk/Erk expression. Values are expressed as the mean ± SEM of three independent experiments. The differential expression between the different conditions was validated by a paired t test *P<0,05, **P<0,01. **B**) mRNA level of DDR1 and DDR2 in a subset of two melanoma cell lines (229 and 238) sensitive (S) or resistant (R) to Vemurafenib. The graph shows the quantification of DDRs mRNA level. Values are expressed as the mean ± SEM of three independent experiments. The differential expression between the different conditions was validated by a paired t test *P<0,05. **C**) Western blotting analysis of DDR1 and DDR2 expression in a subset of two melanoma cell lines (229 and 238) sensitive (S) or resistant (R) to Vemurafenib. GAPDH was used as the endogenous loading control. The graph shows the quantification of DDRs expression. Values are expressed as the mean ± SEM of three independent experiments. The differential expression between the cell lines was validated by a t test *P<0,05. **D**) Western blotting analysis of DDR1 and DDR2 expression in a 229 sensitives cell lines treated with Vemurafenib (10 nM), Cobimetinib (10 nM) or both during 2 months. GAPDH was used as the endogenous loading control.

Figure 2: DDRs role in MAP kinase pathway

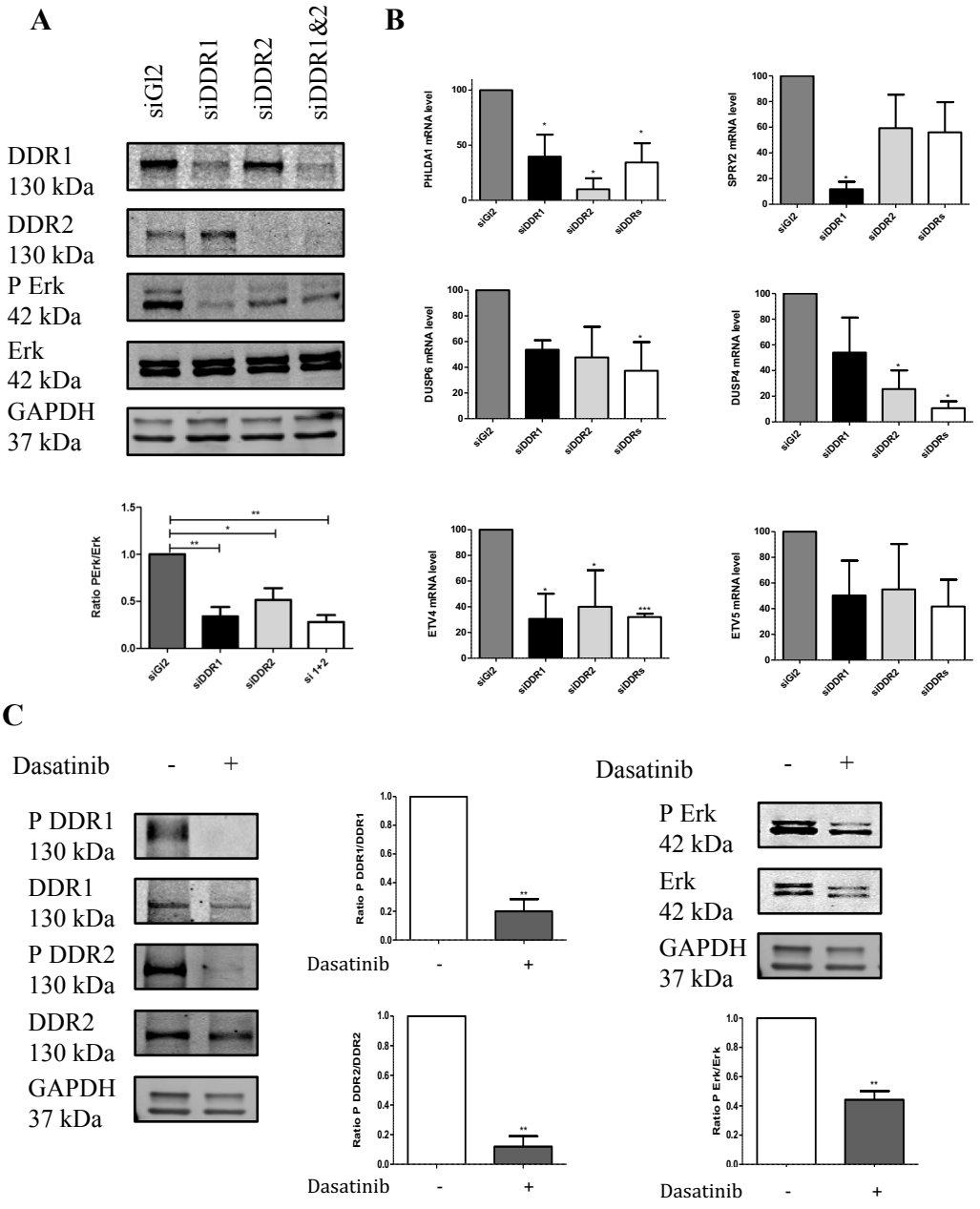

Figure 2: DDRs role in MAP kinase pathway.

A) 238R (left panel) cells were transfected with a siRNA control (siGl2) or targeting DDR1 (siDDR1), DDR2 (siDDR2) or both (siDDR1&2). Protein extracts were then analysed by immunoblotting to determine PErk and Erk expression. GAPDH was used as the endogenous loading control. The graph shows the quantification of PErk/Erk expression. Values are expressed as the mean ± SEM of three independent experiments. The differential expression between the control and the different conditions was validated by a paired t test *P<0,05, **P<0,01. **B**) mRNA level of MAP kinase targets in 238 resistant (R) to Vemurafenib. The graph shows the quantification of PHLDA1, SPRY2, DUSP6, DUSP4, ETV4, ETV5 mRNA level. Values are expressed as the mean ± SEM of three independent experiments. The differential expression between the control and the different conditions was validated by a paired t test *P<0,05, ***P<0,001. **C**) 238R were treated with Dasatinib during 2 hours. Protein extract were then analysed by immunoblotting to determine PErk, Erk, DDR1 and DDDR2 expression. GAPDH was used as the endogenous loading control. The graph shows the quantification of the ratio of PDDR1/DDR1, PDDR2/DDR2 and PErk/Erk. Values are expressed as the mean ± SEM of three independent experiments. The differential expression between the conditions was validated by a paired t test **P<0,01.

Figure 3: DDRs role in proliferation

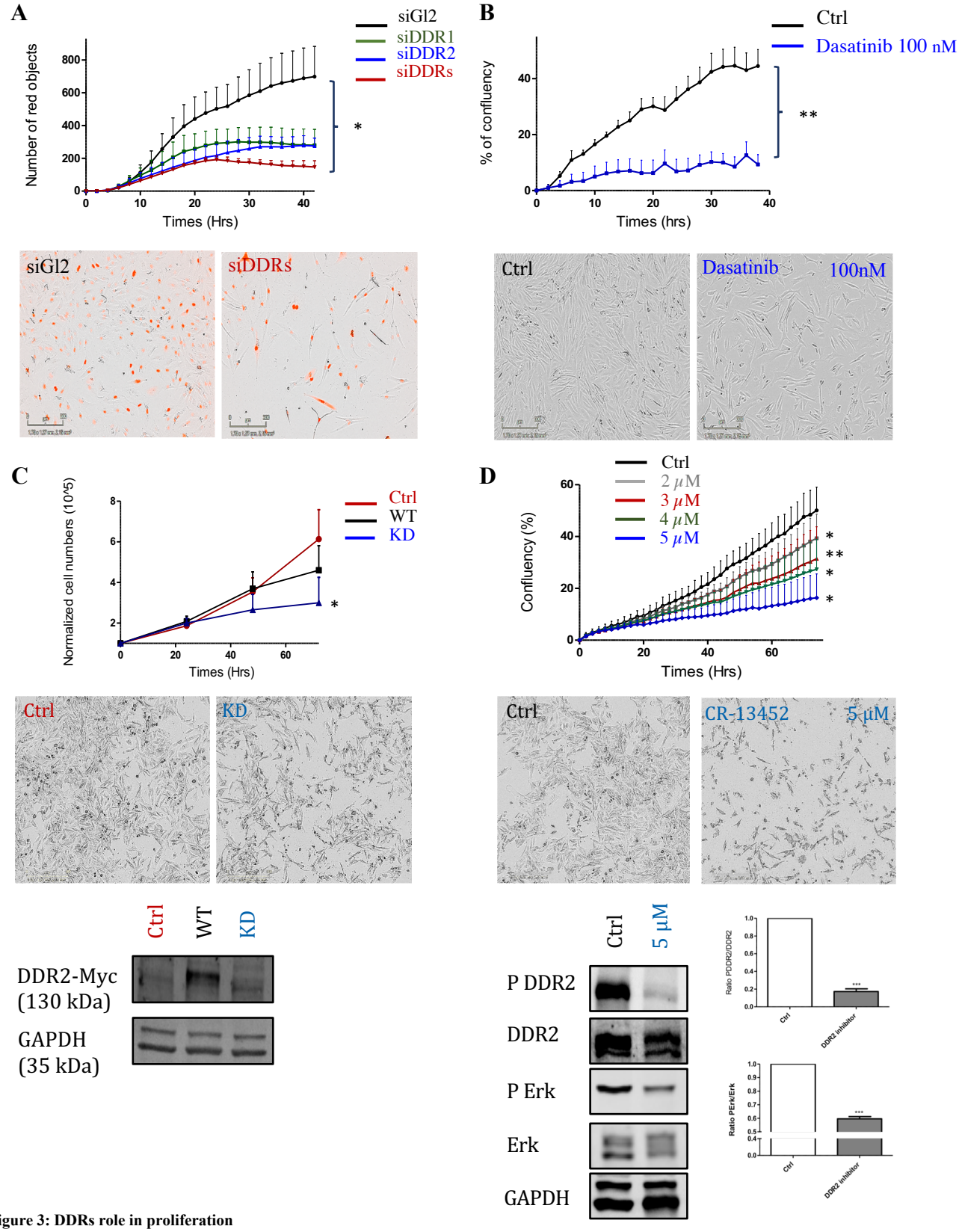

Figure 3: DDRs role in proliferation

A) Incucyte proliferation assay of 238R cells seeded at 5 000 cells per well in a 96 well plate. The cells were transfected with a siRNA control (siGl2) or targeting DDR1 (siDDR1), DDR2 (siDDR2) or both (siDDR1&2). The differential proliferation between the control and the different conditions was validated by a paired t test *P<0,05. **B**) Incucyte proliferation assay of 238R cells seeded at 5 000 cells per well in a 96 well plate cultured in the presence or absence of 100 nM Dasatinib. The differential proliferation between the control and the different conditions was validated by a paired t test **P<0,01. **C**) Proliferation of 229 R cells seeded at 5 000 cells per well in a 96 well plate. The cells were transfected with DDR2 WT-myc or DDR2 KD(K608E)-myc. The differential proliferation between the control and different conditions was validated by a paired t test *P<0,05. Protein extracts were then analysed by immunoblotting to determine DDR2-myc expression. GAPDH was used as the endogenous loading control. **D**) Incucyte proliferation assay of 229R cells seeded at 5 000 cells per well in a 96 well plate cultured in the presence or absence of DDR2 inhibitor. The differential proliferation between the control and different conditions was validated by a paired t test *P<0,05, **P<0,01, ***P<0,001. Protein extracts were then analysed by immunoblotting to determine P DDR2, DDR2, P Erk, Erk expression. GAPDH was used as the endogenous loading control. The graph shows the quantification of the ratio of PDDR2/DDR2 and PErk/Erk. Values are expressed as the mean ± SEM of three independent experiments. The differential expression between the conditions was validated by a paired t test ***P<0,001.

Figure 4: DDRs role in spheroid maintenance

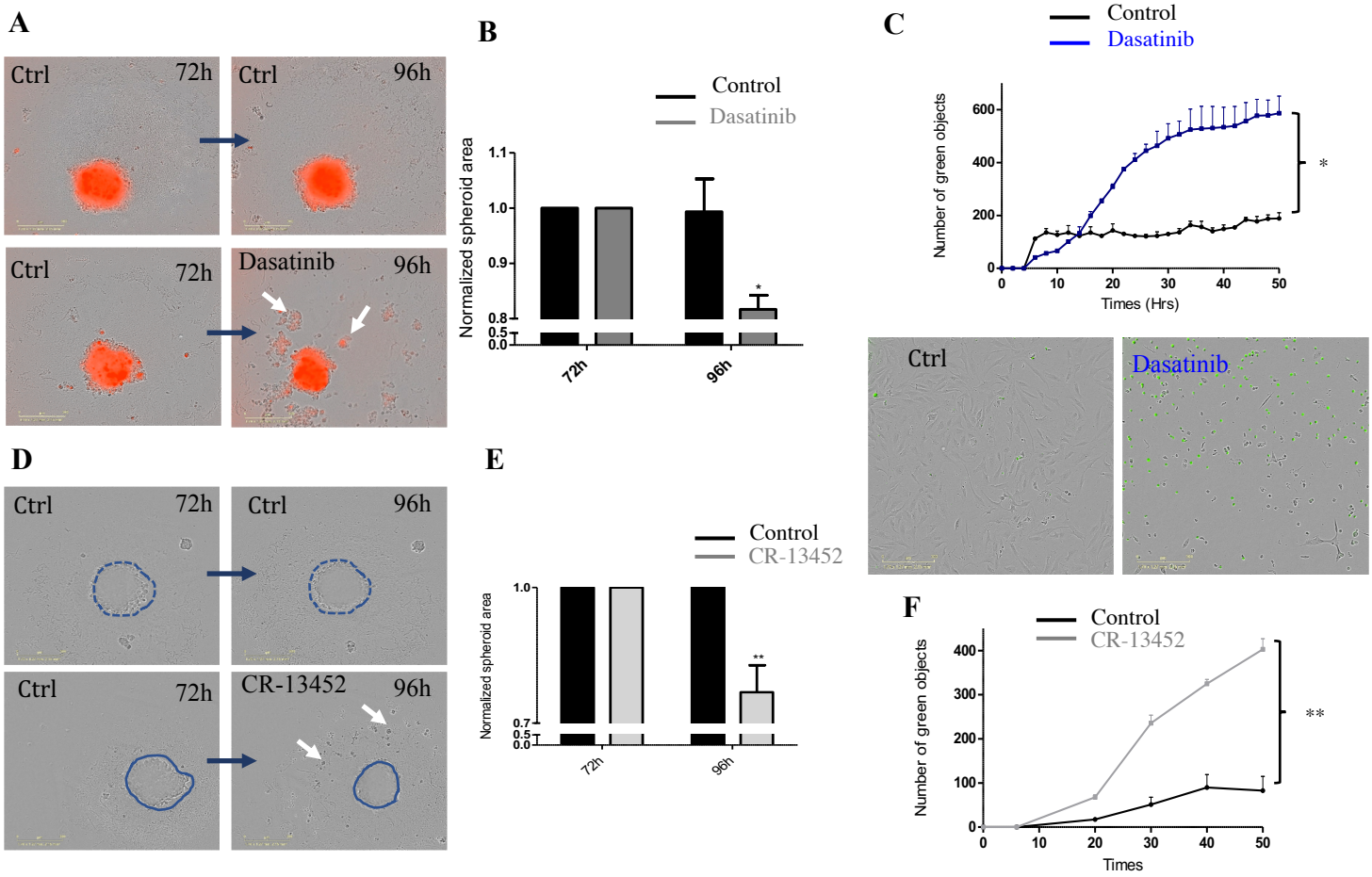

Figure 4: DDRs role in spheroid maintenance

A) 238 R cells were seeded to form spheroids and spheroid at 72 hours were treated with Dasatinib at 100 nM. **B**) The graph shows the quantification of the area in the different conditions. Values are expressed as the mean ± SEM of three independent experiments. The differential area quantification was validated by a paired t test *P<0,05. **C**) Incucyte apoptotic assay of 238R cells seeded at 5 000 cells per well in a 96 well plate cultured in the presence or absence of Dasatinib (100 nM). The differential proliferation between the different conditions was validated by a paired t test *P<0,05. **D**) The Spheroids at 72 hours were treated with DDR2 inhibitor at 5 µM. **E**) The graph shows the quantification of the area in the different conditions. Values are expressed as the mean ± SEM of three independent experiments. The differential area was validated by a paired t test **P<0,01. **F**) Incucyte apoptotic assay of 229R cells seeded at 5 000 cells per well in a 96 well plate cultured in the presence or absence of DDR2 inhibitor (5 µM). The differential proliferation between the different conditions was validated by a paired t test **P<0,01.

Figure 5: DDRs role *in vivo*

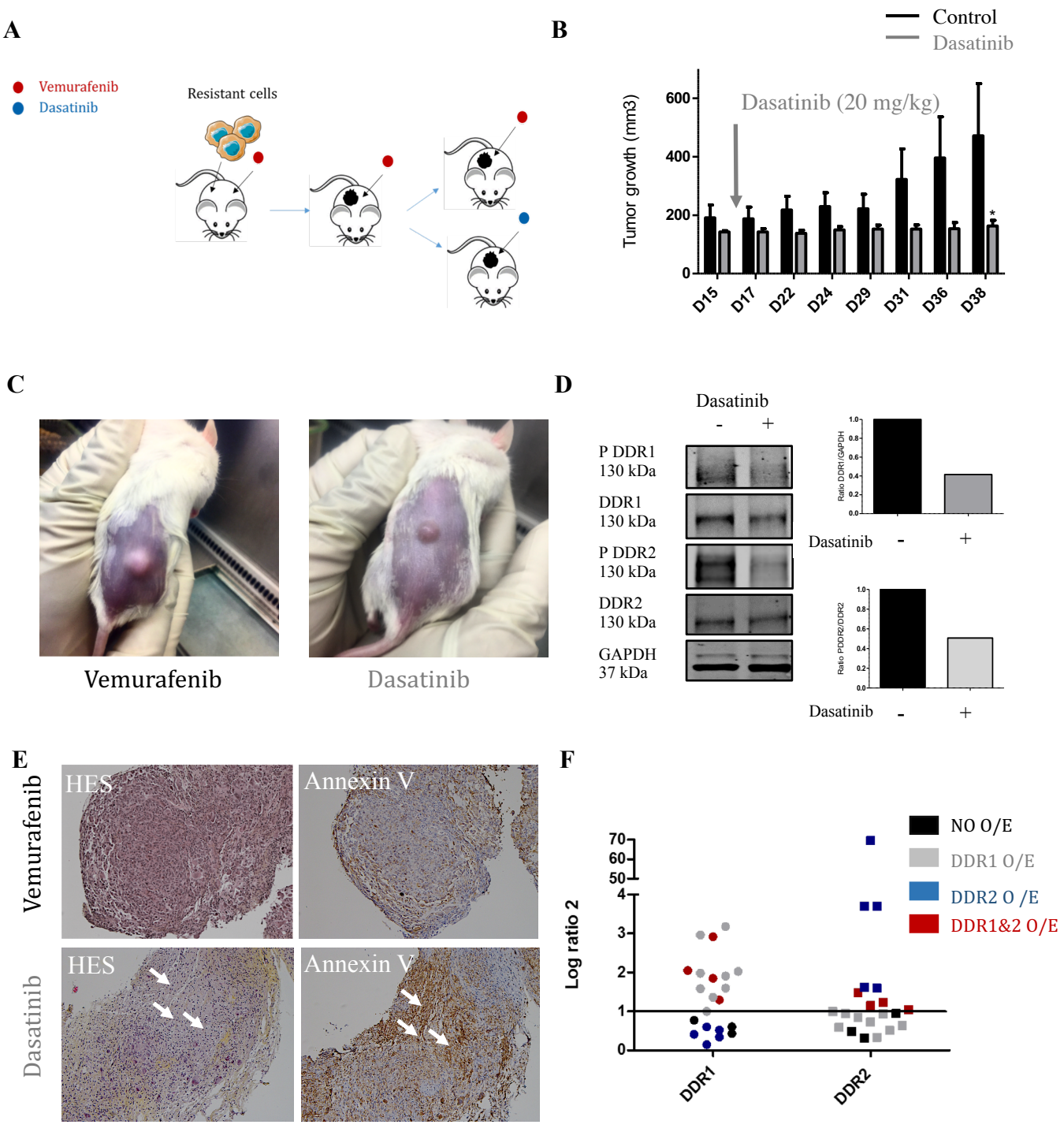

Figure 5: DDRs role *in vivo*

A) 229 R cells ($5*10^6$ cells) were implanted subcutenaously into the left flank of the mouse. When the tumor reached 150 mm^3, the mice were randomly assigned in 2 groups: one control group where the mice are treated with Vemurafenib (40 mg/kg), and the other group where the mice are treated with Dasatinib (20 mg/kg) (n=5 in each condition). **B**) Tumor growth of 229 R in the left flank of NOG mice subcutaneously injected with $5*10^6$ 228R cells. **C**) Pictures of mice treated with Vemurafenib or Dasatinib. **D**) Western blotting analysis of DDR1 DDR2, PDDR1, PDDR2 expression in mouse primary tumor treated or not with Dasatinib. GAPDH was used as the endogenous loading control. The graph shows the quantification of the ratio of PDDR1/DDR1, PDDR2/DDR2. **E**) Immunohistochemistry of mouse primary tumor treated or not with Dasatinib. Left panel : HES of mouse primary tumor. Right panel: Immunostaining of Annexin V. **F**) RNA sequencing data for DDR1 or DDR2 abundance after treatment to an anti-BRAF. All the dots above the black lines, meaning that there is an increase of receptor's abundance after treatment (in grey if DDR1 is overexpressed, in blue if DDR2 is overexpressed, in red if DDR1 and 2 are overexpressed).

Supplementary figure 1: DDRs role in MAP kinase pathway

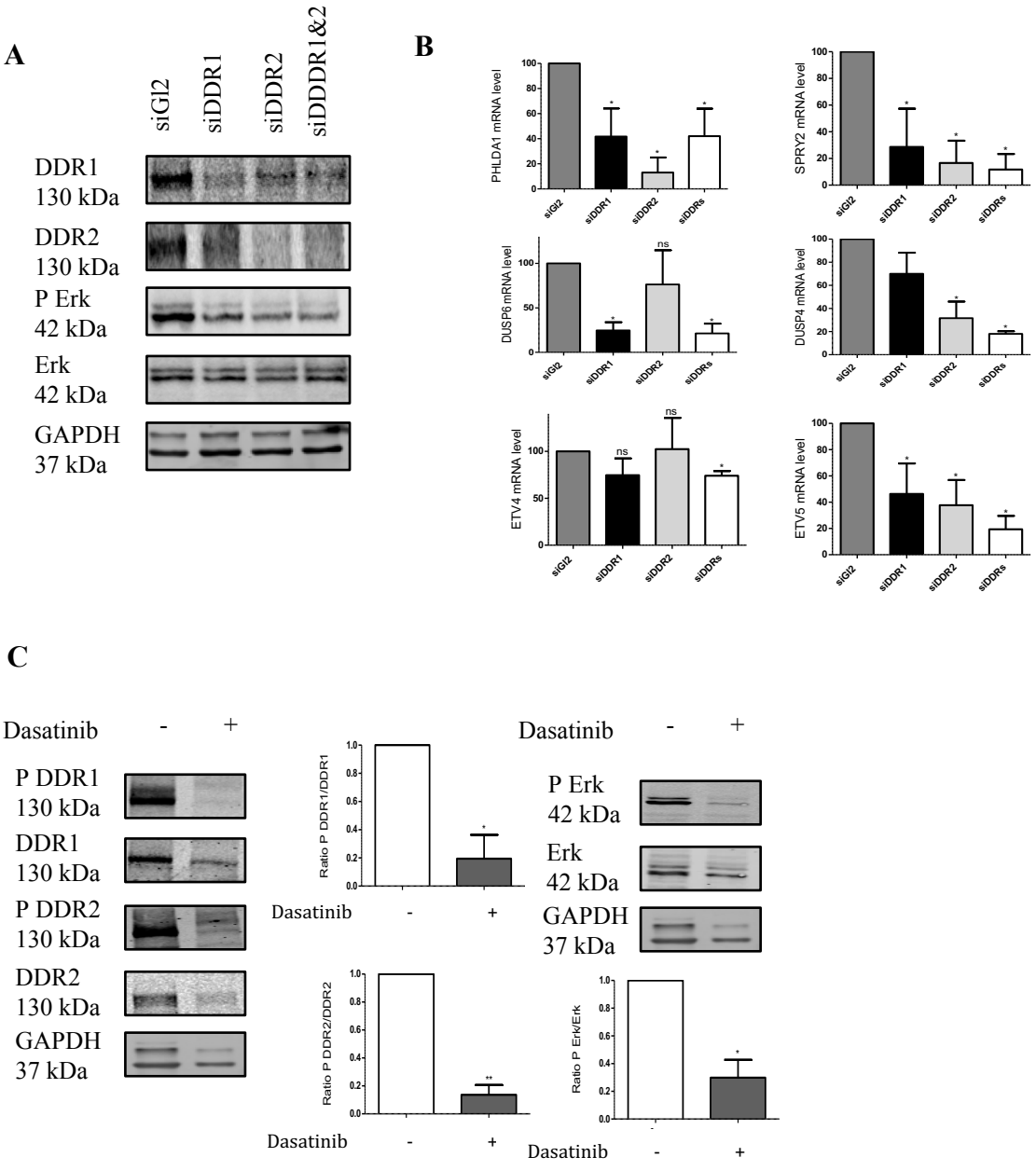

Supplementary figure 1: DDRs role in MAP kinase pathway.
A) 229R cells were transfected with a siRNA control (siGl2) or targeting DDR1 (siDDR1), DDR2 (siDDR2) or both (siDDR1&2). Protein extracts were then analysed by immunoblotting to determine PErk and Erk expression. GAPDH was used as the endogenous loading control. **B**) mRNA level of MAP kinase targets in 229 resistant (R) to Vemurafenib. The graph shows the quantification of PHLDA1, SPRY2, DUSP6, DUSP4, ETV4, ETV5 expression. Values are expressed as the mean ± SEM of three independent experiments. The differential mRNA level between the control and different conditions was validated by a paired t test *P<0,05. **C**) 229R were treated with Dasatinib during 2 hours. Protein extract were then analysed by immunoblotting to determine PErk and Erk expression. GAPDH was used as the endogenous loading control. The graph shows the quantification of the ratio of PDDR1/DDR1, PDDR2/DDR2 and PErk/Erk. Values are expressed as the mean ± SEM of three independent experiments. The differential expression between the conditions was validated by a paired t test *P<0,05, **P<0,01.

Supplementary figure 2: DDRs role in proliferation

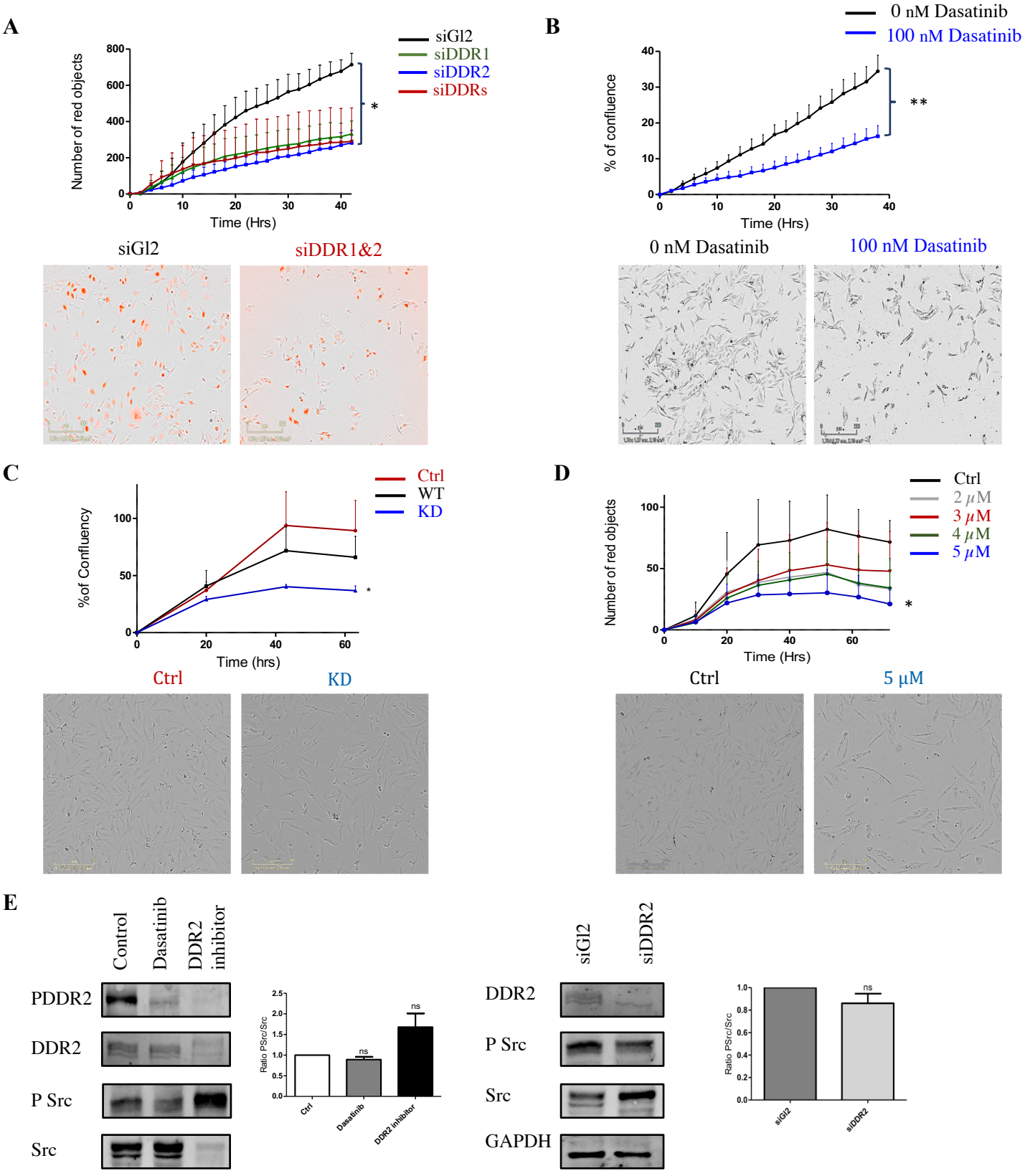

Supplementary figure 2: DDRs role in proliferation

A) Incucyte proliferation assay of 229 R cells seeded at 5 000 cells per well in a 96 well plate. The cells were transfected with a siRNA control (sGl2) or targeting DDR1 (siDDR1), DDR2 (siDDR2) or both (siDDR1&2). The differential proliferation between the different conditions was validated by a paired t test *P<0,05. **B**) Incucyte proliferation assay of 229R cells seeded at 5 000 cells per well in a 96 well plate cultured in the presence or absence of 100 nM Dasatinib. The differential proliferation between the control and the different conditions was validated by a paired t test **P<0,01. **C**) Proliferation of 238R cells seeded at 5 000 cells per well in a 96 well plate. The cells were transfected with DDR2 WT-myc or DDR2 KD(K608E)-myc. The differential proliferation between the control and the different conditions was validated by one way anova *P<0,05. **D**) Incucyte proliferation assay of 238R cells seeded at 5 000 cells per well in a 96 well plate cultured in the presence or absence of DDR2 inhibitor. The differential proliferation between the control and the different conditions was validated by a one way anova *P<0,05. **E**) 238R were transfected with a siRNA control (siCtrl) or targeting DDR2 (siDDR2) or treated with DDR2 inhibitor during 72 hours. 238R cells were treated with Dasatinib during 2 hours. Protein extract were then analysed by immunoblotting to determine PErk, Erk, PAkt and Akt expression. Protein extracts were analysed by immunoblotting to determine P DDR2, DDR2, P Src, Src expression. GAPDH was used as the endogenous loading control. The graph shows the quantification of the ratio of PSrc/Src. Values are expressed as the mean ± SEM of three independent experiments. The differential expression between the conditions was validated by a one way anova or a paired t test: ns: non significant.

Supplementary figure 3: GSEA analysis

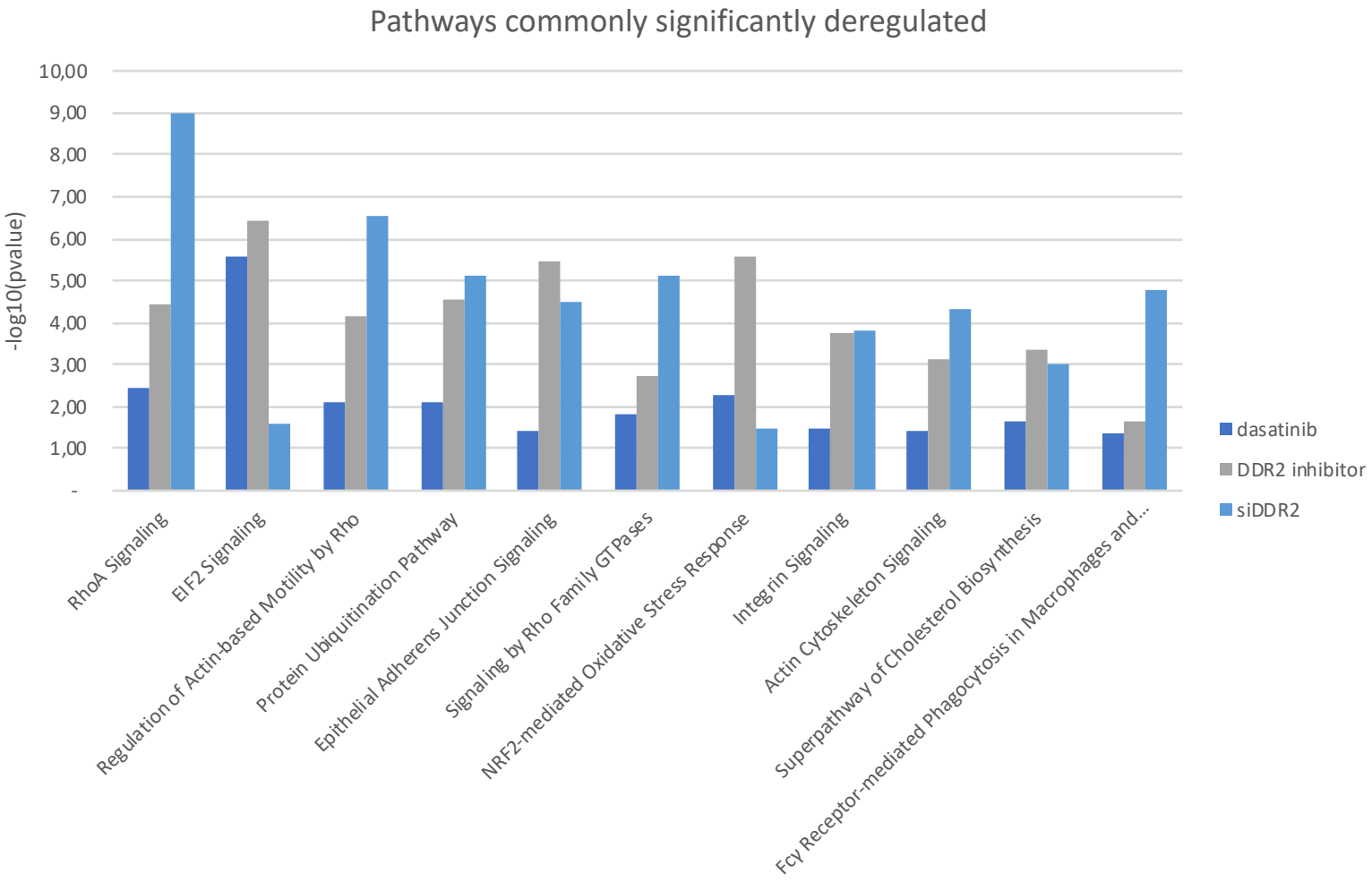

Supplementary figure 3: GSEA analysis
Pathways commonly and significantly enriched between the following conditions: 238R cells treated with dasatinib, with a DDR inhibitor or transfected with siRNA targeting DDR2. Gene set enrichment analysis (GSEA) was performed against the Ingenuity Pathways database (fisher test expressed in -log10pvalue).

Supplementary figure 4: DDRs role in spheroid maintenance in 229R

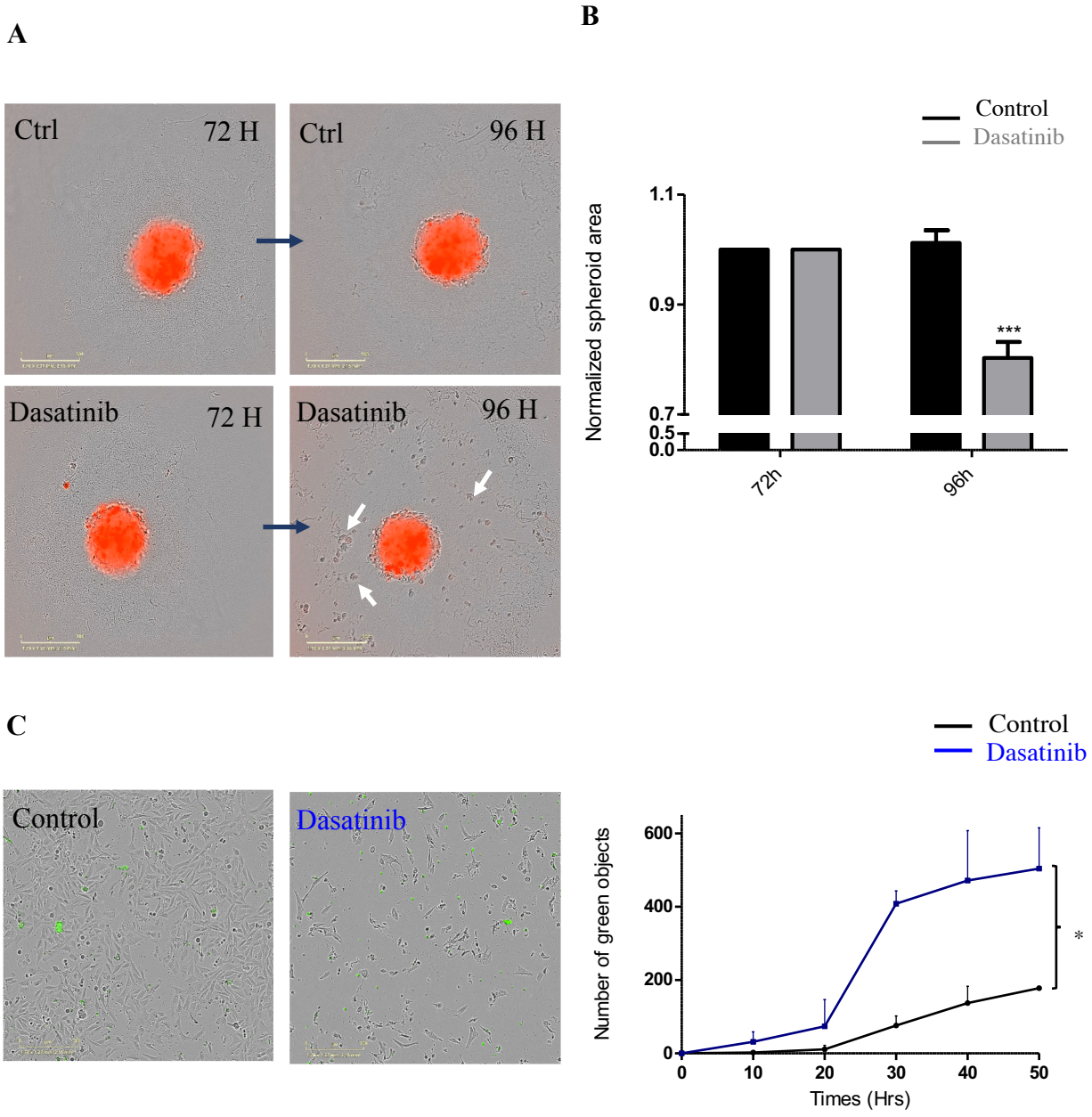

Supplementary figure 4: DDRs role in spheroid maintenance in 229R

A) 229 R cells were seeded to form spheroids and spheroid at 72 hours were treated with Dasatinib at 100 nM. **B**) The graph shows the quantification of the area in the different conditions. Values are expressed as the mean ± SEM of three independent experiments. The differential expression was validated by a paired t test ***P<0,001. **C**) Incucyte apoptotic assay of 229R cells seeded at 5 000 cells per well in a 96 well plate cultured in the presence or absence of Dasatinib (100 nM). The differential proliferation between the different conditions was validated by a paired t test *P<0,05.

Supplementary table 1: PCR primers

Gene	Forward primer (5'→ 3')	Reverse primer (5'→3')
DDR1	CCG ACT GGT TCG CTT CTA CC	CGG TGT AAG ACA GGA GTC CAT C
DDR2	GAG GAG CGC TTA TGA TCC TGA TTC CC	TAT ACC CGG GAC TCG TCG CCT TGT TG
PHLDA1	GAAGATGGCCCATTCAAAAGCG	GAGGAGGCTAACACGCAGG
SPRY2	CCTACTGTCGTCCCAAGACCT	GGGGCTCGTGCAGAAGAAT
DUSP6	GAAATGGCGATCAGCAAGACG	CGACGACTCGTATAGCTCCTG
DUSP4	GGCGGCTATGAGAGGTTTTCC	TGGTCGTGTAGTGGGGTCC
ETV4	CAGTGCCTTTACTCCAGTGCC	CTCAGGAAATTCCGTTGCTCT
ETV5	CAGTCAACTTCAAGAGGCTTGG	TGCTCATGGCTACAAGACGAC